ELECTRON CAPTURE BY LOW-ENERGY HIGHLY-CHARGED

NEON PROJECTILES FROM HELIUM ATOMS

STUDIED BY ENERGY-GAIN SPECTROSCOPY

by

CHRIS MICHAEL SCHMEISSNER

B.S., Kansas State University, 1981

A MASTER'S THESIS

submitted in partial fulfillment of the

requirements for the degree

MASTER OF SCIENCE

Department of Physics

KANSAS STATE UNIVERSITY

1983

Approved by:

C L Cocke

Major Professor

TABLE OF CONTENTS

Page

LIST OF TABLES

LIST OF FIGURES

Figure | Page

ACKNOWLEDGEMENTS

I would like to express my love and affection to my parents and sister for their never ending love and support.

To Dr. C. L. Cocke I wish to express my deepest gratitude. His foresight and patience made this work possible. With great respect I give him many thanks.

I would like to acknowledge the help provided by Dallas Kingsbury in developing computer programs for data reduction.

I would also like to thank J. Shinpaugh, G. Euliss and W. Waggoner for their friendship and support.

For the excellent job done in typing the thesis I thank KoKo Himes.

In closing I wish to express my love to my newlywed wife, Baretta, and her family for their immeasurable support.

I acknowledge the financial support of the U.S. Department of Energy.

THIS BOOK CONTAINS NUMEROUS PAGES WITH THE ORIGINAL PRINTING BEING SKEWED DIFFERENTLY FROM THE TOP OF THE PAGE TO THE BOTTOM.

THIS IS AS RECEIVED FROM THE CUSTOMER.

Chapter I

INTRODUCTION

In recent years a great deal of effort has been made in the area of atomic collisions to increase the understanding of the electron capture reaction. The ability to produce highly charged ions in a velocity range of 10^6 - 10^7 cm/s has enabled the capture process of highly charged ions to be studied in a velocity regime which had been relatively untouched by theory or experiment. In the capture process one or more electrons from a neutral target are transferred into an atomic level of the highly charged projectile ion. In these collisions the projectile ion moves slowly in comparison to the orbital velocities of the target electrons. The slow evolution of the electron cloud due to the slow moving projectile ion makes a quantum mechanical description difficult. Quantum mechanical models for low velocity collisions which account for partially stripped projectiles and many electron targets, where the interactions among all electrons have to be taken into consideration, are rare. Simplifying assumptions have been formulated for many models, and these models require experimental results for comparison. This work was done in order to provide a greater understanding of the physics involved in capture involving low energy highly charged projectiles.

Areas of interest are not only limited to the physics of the collision process, but applications also exist in the area of controlled thermonuclear fusion research. These low velocity collisions are significant in magnetically confined high temperature plasmas. The low energy highly charged ions can capture a hydrogen electron into an excited state and radiatively decay, causing cooling of the plasma.[1,2]

A general feature of the low velocity high charge Ne^{+q} + He collision system is the exoergicity of the capture reaction. Capture for this system takes place into an excited level. The change in internal energy of the colliding system is converted into kinetic energy. This thesis presents a study of electron capture by examining the energy-gained by the projectile ion. The measured energy-gain enables the determination of the populated energy levels of the projectile ion. Energy-gain spectra for Ne^{+q} (q=3-8) on He, at projectile energies from (71.69 eV)·q to (523.53 eV)·q were obtained. Combining these spectra with the capture cross sections of Justiniano[3] and Cocke et al.[4] results in a greater understanding of the collision process.

Chapter II of this thesis presents experimental techniques in data acquisition and analytical methods used to produce the energy-gain spectra. The experimental results are presented in Chapter III. Chapter IV contains two theoretical models used to explain the collision process. A discussion of the results are presented relative to the models in Chapter V. The conclusions drawn from these results are given in Chapter VI.

Chapter II

EXPERIMENT

A. Experimental Apparatus

(1) Production of Low-Energy Highly Charged Ions

Beams of F^{+4}, F^{+5} and a foil poststripped beam of I^{+5} ions from the Kansas State University EN tandem Van de Graaff accelerator were passed through a cell containing neon gas. The poststripped iodine beam was used for its larger charge state so as to produce a greater number of the higher recoil charge states. The apparatus is shown in Figure 1. The chamber was kept at pressures on the order of 2×10^{-6} torr. The neon recoil ions, also called projectile ions, were extracted perpendicular to the incident beam by an electric field. The voltages V_1 and V_2 were set so as to optimize the resolution and transmission of the detected ions. Typical voltages of V_1 and V_2 were 29 and 8 volts, yielding accelerated energies close to $qe \cdot V_1$, e being one electron charge and q the charge state.

The various charge states of the projectile ions were separated due to their different charge-to-mass ratios by being passed through a 180^0 double-focusing magnet with a mean radius of 7.5 cm and a momentum resolution of 1.2%.[5] The projectile ions then passed through a second gas cell which was at a voltage V_c. The second cell contained helium gas whose pressure was monitored by a capacitance manometer and was typically 1.3 mTorr. The projectile ions were then analyzed by a 180^0 double-focusing hemispherical electrostatic spectrometer and detected by a channeltron. The voltage of the spectrometer plates was fixed so as to pass only ions with certain

Figure 1: Schematic of experimental apparatus.

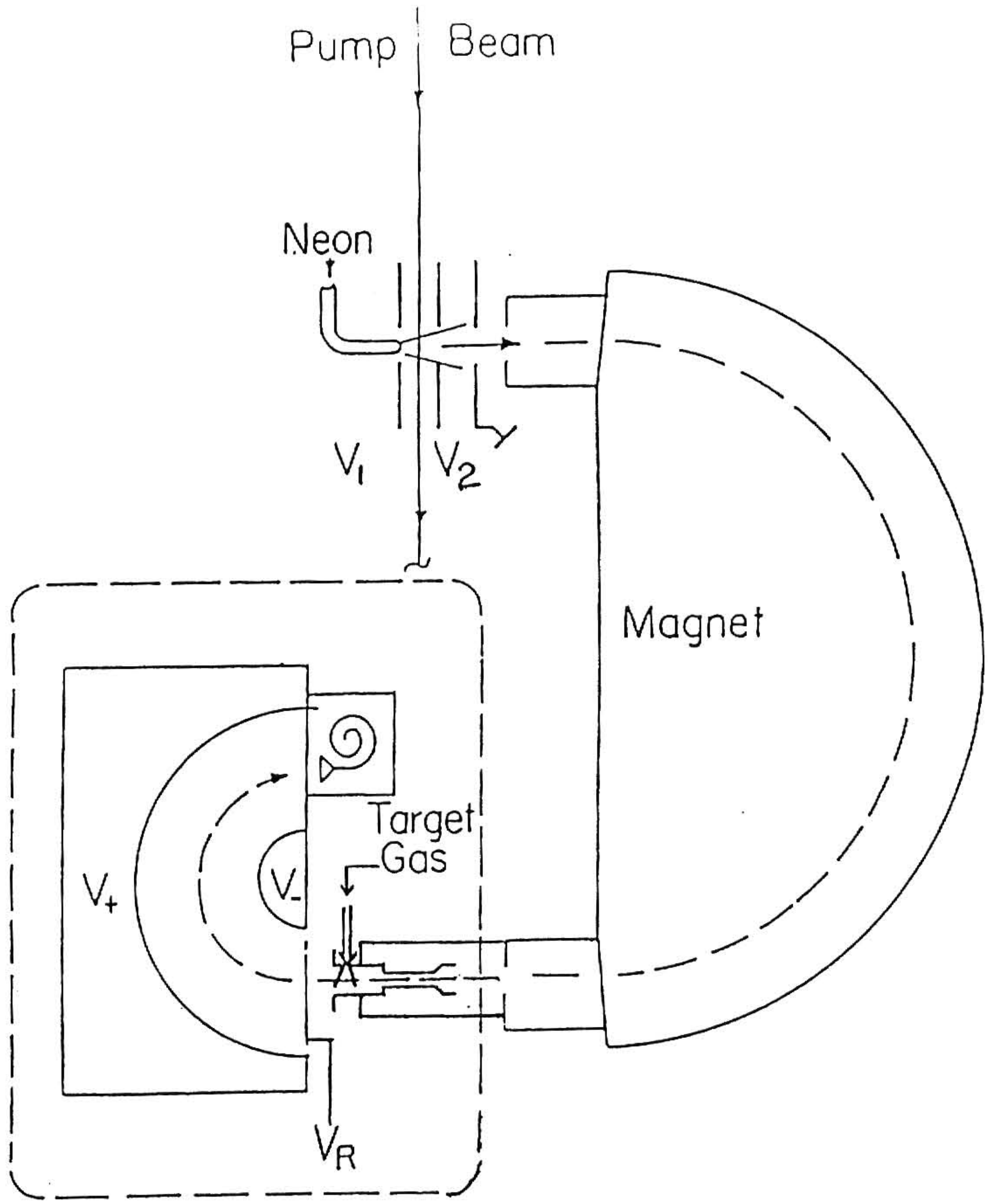
Pump Beam
Neon
V1
V2
Magnet
Target
Gas
V+
V-
VR

energy per charge, typically 12 eV/q. At the entrance slit (2x4 mm) of the spectrometer a triangle wave generator produced a scanning retardation voltage which slowed the ions until the proper energy was reached for the ions to pass through the spectrometer. Upon detection of the projectile ion at the channeltron the retardation voltage was sampled (Figure 2).

B. Data Analysis

(1) Experimental Determination of Energy-Gain

The potential difference, ΔV, of the analyzer for which the spectrometer passes an ion is directly proportional to the ion's energy, E, and inversely proportional to the charge state q. If the energy and charge state leaving the second gas cell change to E' and q' respectively due to a charge-exchange reaction in the second cell, one has the two equations:

$$\Delta V = K \frac{E}{q} \tag{1a}$$

$$\Delta V = K \frac{E'}{q'} \tag{1b}$$

where K is a constant depending on the geometry of the analyzer (Appendix A). The energies E and E' are given by

$$E = (V_o + V_c)q - (V_R^o + V_c)q \tag{2a}$$

$$E' = (V_o + V_c)q - (V_R + V_c)q' + E_G \tag{2b}$$

where V_o is the effective accelerating voltage in the primary cell, a voltage $-V_c$ is applied to the second gas cell, V_R^o and V_R are the voltages needed to retard the direct and charge-exchange beams respectively to allow them to pass through the analyzer, and E_G is the energy given to the projectile in the capture reaction. Solving the equations for E_G yields

Figure 2: Electronics block diagram for energy-gain experiment.

Electronics

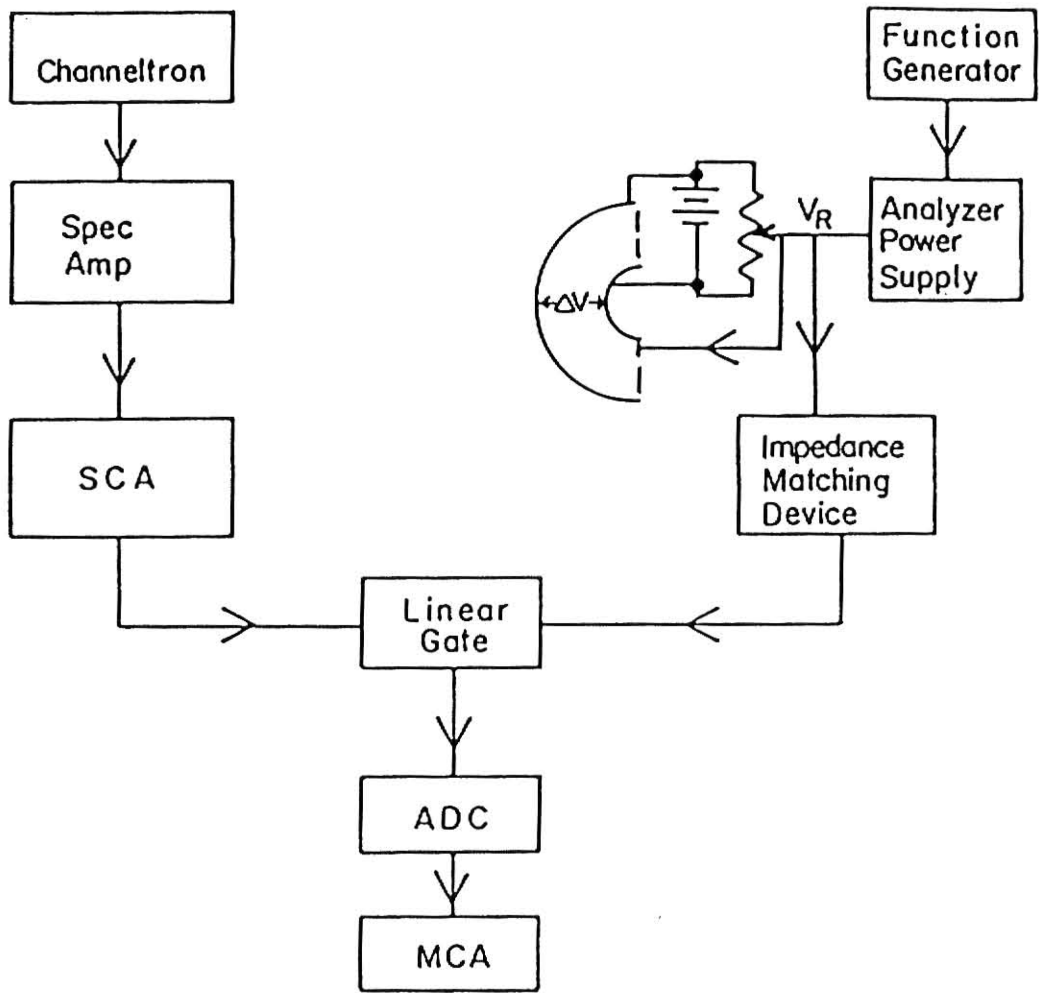

$$E_G = q'(V_R - V_R^o) + (V_o + V_c)\,(q' - q). \tag{3}$$

Equation (3) gives the relationship between the retarding voltage and the energy-gain. This enables the spectrum of events measured as a function of retarding voltage to be converted to an energy-gain spectrum. Since ion energy at impact is $q(V_o + V_c)$, we define $V_{acc} \equiv (V_o + V_c)$ and label our figures by this parameter.

The value of K was determined using the following:

$$V_o = \frac{\Delta V}{K} + V_R^o. \tag{4}$$

The effective accelerating voltage V_o was held constant and the values of ΔV and V_R^o were varied to allow direct beam to pass through the system. A plot of ΔV versus V_R^o will yield a line with a slope of 1/K and an intercept of V_o. A digital voltmeter was used to monitor ΔV and V_c to 1/100 of a volt.

An adapted version of a standard SCIPLOT plotting program (Appendix B) was modified to operate as follows. The initial charge state q, the charge-exchange state q', ΔV, V_c and K were input into the program. The program located the channel number of V_R^o by finding the centroid of the direct beam. From this a value of V_o was obtained using Equation (4). Combining $V_{acc} \equiv (V_o + V_c)$ and Equation (3) we become able to determine a value of E_G for each channel number.

(2) Kinematics

The energy-gained by the incident projectile in the capture process is a function of scattering angle and Q-value, where Q is the difference between the initial and final electronic energies for capture into a given final level. To understand the collision process better we can define a quantity

R_c called the crossing radius for capture. The crossing radius is the internuclear distance between the projectile and target where the electronic energy of the initial system is equal to that of the final one. In a level crossing model for capture, this is the radius at which the target electron will be transferred to the projectile ion. If polarization effects are ignored, this gives $R=(q-1)e^2/Q$ for single capture. Thus a system with a large Q-value will have a small crossing radius. A collision with a large crossing radius will impart a negligible amount of energy to the target. We can then assume the energy-gained will be equal to the Q-value of the reaction. However at low projectile velocities ($< 10^6$ cm/s) the larger the exoergicity of the Q-value the greater the energy carried off by the target at the expense of the projectile energy. In an effort to represent this kinematic effect, each spectrum has superimposed on it a plot of energy-gain versus scattering angle of the projectile (Figure 3). The kinematic curves were calculated using the computer programs KINEMA and KINEMA1 (Appendix C), which utilize standard Rutherford scattering equations derived from conservation of energy and momentum.[6] Only a portion of the kinematic curve is represented in each spectra. This region of interest corresponds to collisions occurring at distances of closest approach lying between one crossing radius and one-half crossing radius. This region represents roughly 3/4 of the total cross section. Large kinematic shifts will result in peaks severely skewed and shifted to lower energies. With the use of these curves it becomes obvious that the kinematic curve for a given level must lie inside the populated peak.

(3) Finite Angular Acceptance of the Spectrometer

The acceptance geometry of the system can be represented in two

Figure 3: Energy-gain spectrum for Ne^{+6} at an acceleration voltage of 124.17.

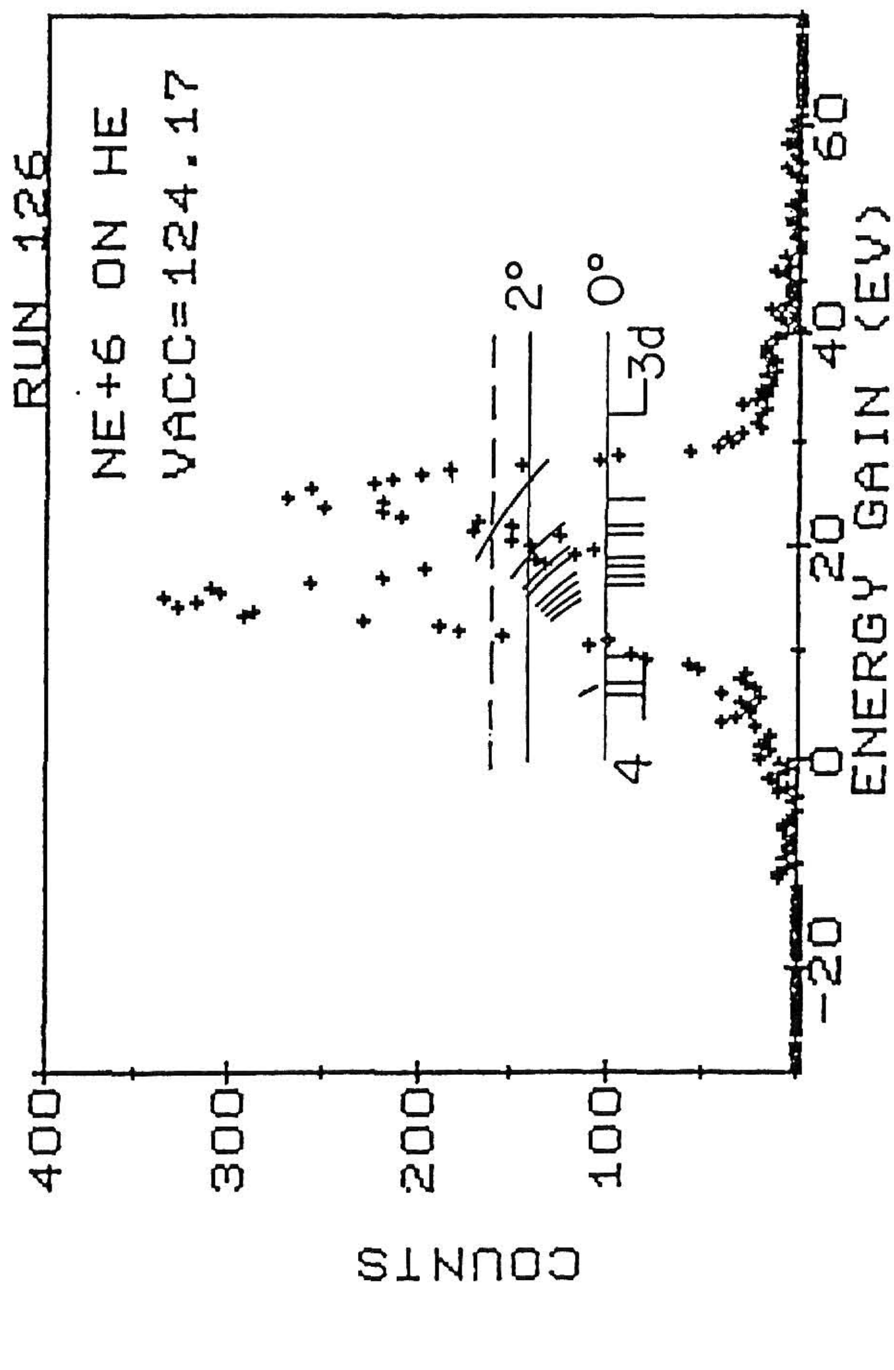
RUN 126
NE+6 ON HE
VACC=124.17
2°
0°
3d
4
COUNTS
400
300
200
100
-20
0
20
40
60
ENERGY GAIN (EV)

sections, lableled A and B in Figure 4a. Section A consists of a three grid system at the entrance of the spectrometer. Section B depicts the secondary gas cell and a focusing plate at the cell's entrance. To determine the focusing properties of the entire system (A and B) we shall concentrate on each section individually.

Figure 4a shows that the retarding voltage V_R is applied to the entrance plate of the spectrometer (Section A). The preceding two grids are held at ground potential and a voltage $-V_c$. The focusing properties were explored using an optics program which numerically determines a potential for a given geometry. The voltages on the entrance grid range from 50 volts to a maximum of 500 volts. By considering a point source emanating from inside the gas cell the program showed that events scattered by more than $\theta_c=2.8^o$ were not passed by the retardation system. This value of θ_c is virtually independent of the voltage on the first plate ($50 \leqslant V_R \leqslant 500$). This fact is due to the small spacing between the the three grids. In this projectile energy range the small plate spacing doesn't allow the ion time to move laterally due to the electric fields. Thus the angular acceptance of the 3 grid system is around 2.8^o virtually independent of retarding voltage. The projectile path is represented in Figure 4b.

The range of voltage swept by V_R is also applied to the gas cell of Section B. The uncertainty in the properties of the beam leaving the magnet make it extremely difficult to quantitatively determine the trajectory of the projectile. However calculations revealed some gross features:

(1) The gas cell focuses the beam to a point inside the cell.

(2) The focal point depends upon the retarding voltage. An increase in V_R results in moving the focal point closer to the cell entrance.

Figure 4a: Schematic of secondary gas cell and spectrometer entrance grids.

Figure 4b: Various projectile paths (labeled 1,2,4,5) through the spectrometer entrance grids. The initial energy of the projectiles was 510 eV. Each was retarded by 500 eV to an energy of 10 eV. The labeled angles denote the angle at which the projectile left the point source.

ILLEGIBLE DOCUMENT

THE FOLLOWING DOCUMENT(S) IS OF POOR LEGIBILITY IN THE ORIGINAL

THIS IS THE BEST COPY AVAILABLE

P-474

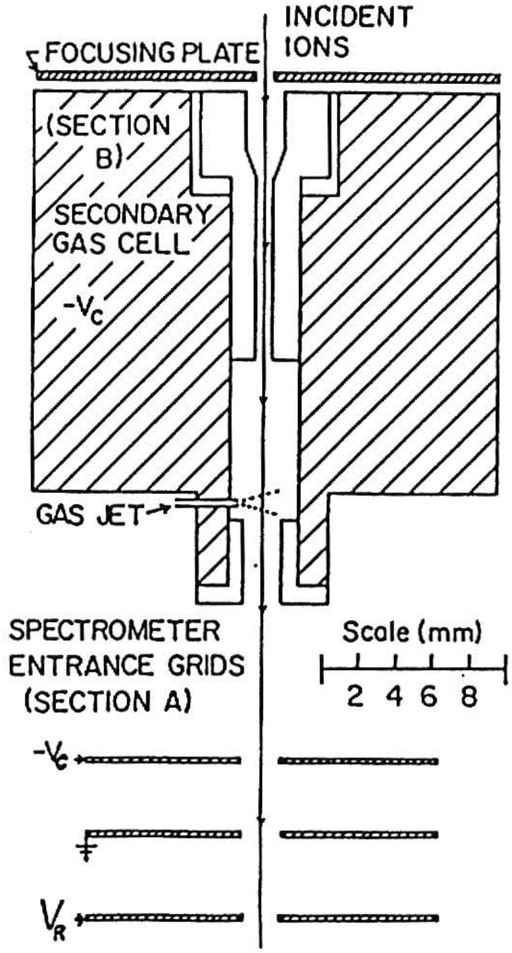
INCIDENT
IONS
FOCUSING PLATE
(SECTION
B)
SECONDARY
GAS CELL
$-V_c$
GAS JET
SPECTROMETER
ENTRANCE GRIDS
(SECTION A)
Scale (mm)
2 4 6 8
$-V_c$
V_R

(a)

(b)

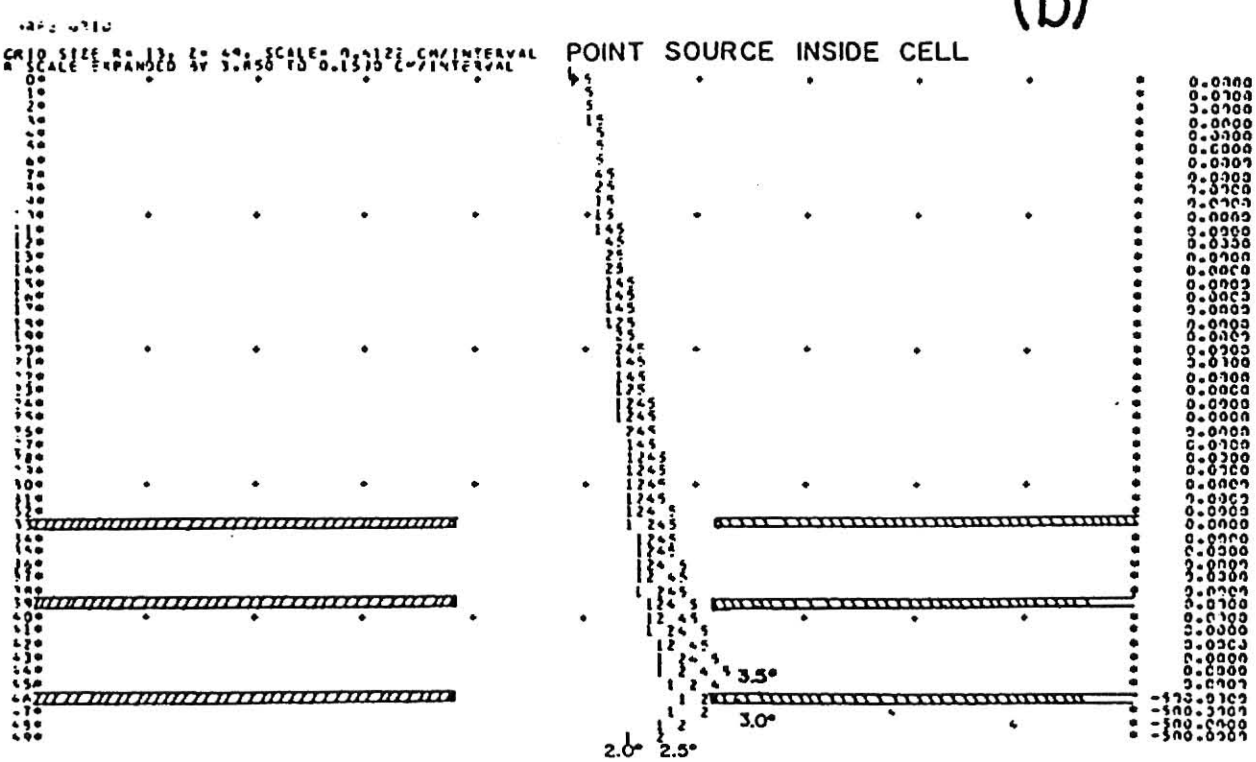
POINT SOURCE INSIDE CELL
3.5°
3.0°
2.0°
2.5°

Due to uncertainty in the properties of the beam leaving the magnet a total understanding of the trajectory through the entire system is difficult. For the lowest V_R (70 and 120 V) it appeared that the effects of system B were relatively small and cutoff angle of 2.8^0 is appropriate. For the larger acceleration voltages, the angular distribution becomes washed out by the incident beam divergence, and a larger θ_c obtains. However for the larger V_R, reaction products are directed more in the forward direction so that the importance of knowing the exact value of θ_c is reduced. In drawing the figures, we have adopted a universal θ_c of 2.8^0.

Experimental evidence for this angular cutoff is seen in Figures 3 and 5. In the Ne^{+6} spectra (V_{acc} = 124.17) a sharp cutoff for the 3d state is observed near 2.8^0. This same sharp cutoff also present in the Ne^{+4} spectra (V_{acc} = 72.09) for the 3s states.

(4) Spectral Resolution

The overall energy resolution of the system is reflected in the energy width of the direct-energy beam. The major contributions to peak width were: (1) a spread of energies in the incident beam, (2) the finite sizes of the entrance and exit slits of the spectrometer, and (3) the kinematic spread and the population of overlapping levels.

From the direct beam (Q=0) the peak width, δE_G, in the energy-gain plot can be calculated on first principles by (Appendix D)

$$(\delta E_G)^2 = (\delta E_S)^2 + (\delta E_b)^2 \qquad (5)$$

where δE_S is the resolution of the spectrometer and δE_b is the energy resolution of the incident beam. The energy resolution, δE_b, is found by multiplying the energy resolution of the magnet by the incident energy.

Figure 5: Energy-gain spectrum for Ne^{+4} at an acceleration voltage of 72.09.

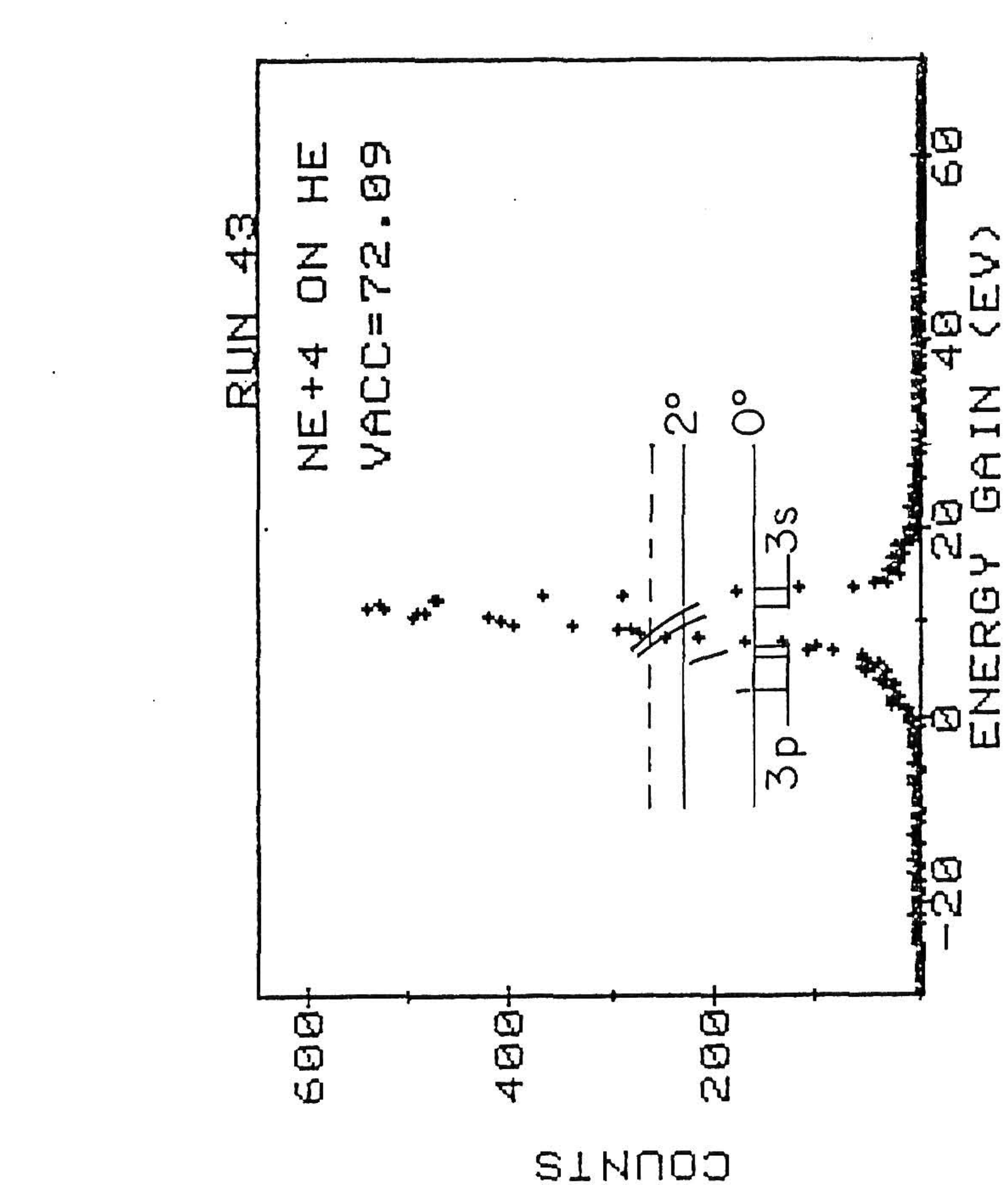
RUN 43
NE+4 ON HE
VACC=72.09
2°
0°
3p
3s
ENERGY GAIN (EV)
-20
0
20
40
60
COUNTS
200
400
600

The momentum resolution was found to be $\Delta P/P = 1.2\%$ yielding an energy resolution of $\Delta E/E = 2.4\%$. The projectile energy extracted from the low-energy high charge source was (25 eV)$\cdot$q. These values give a result for δE_b of (0.62 eV)$\cdot$q.

The resolution of the spectrometer is also the product of the energy resolution, $\Delta E/E$, and the projectile energy after retardation. It can be shown for the analyzer, $\frac{\Delta E}{E} = \frac{\Delta r}{2r}$, where Δr is the analyzer slit width and r is the mean radius of the spectrometer. This result is $\Delta E/E = 3\%$. The energy of the retarded projectile is near (12 eV)$\cdot$q. The above yields a value of (0.36 eV)$\cdot$q for δE_S. Using Equation (5) we find δE_G = (0.72 eV)$\cdot$q. Typical measured values for main peak width range from (0.8 eV)$\cdot$q to (0.4 eV)$\cdot$q. It is found for higher cell voltages ($V_c \gtrsim 200$ volts) δE_G increases to (2 eV)$\cdot$q. This is presumably due to aberrations in the analyzer and some reactions occuring in between the cell and the spectrometer entrance.

The resolution of the capture beam can also be evaluated by an equation similar to that of Equation (5) (Appendix D)

$$(\delta E_G')^2 = \left(\frac{q'}{q}\right)^2 (\delta E_S)^2 + (\delta E_A)^2 \tag{6}$$

where q' is charge state of the capture beam. The best method for evaluation of the single capture peak is to use the approximation $q \approx q'$. The measured width of the main peak will then be the width expected for the single capture peak (with no kinematic spread). For this reason all plots show a direct as well as a capture peak as a measure of the resolution function.

(5) Calculation of Q-Values

The difference between the initial and final electronic energies for capture into a given final level is unique and defines the Q-value for that reaction channel. As an example of how Q was calculated, a schematic of the initial and various final levels for the system $Ne^{+3} + He \rightarrow Ne^{+2*} + He^{+}$ is shown in the energy level diagram of Figure 6.

The Q-value is obtained by the following equations:

$$Q = -IP(He) + BE(Ne^{+2*}) \tag{7a}$$

$$= -IP(He) + IP(Ne^{+2}) - Ex(Ne^{+2}) \tag{7b}$$

where IP, BE and Ex are the ionization potentials, binding energies and excitation levels of the bracketed quantities. Values for each of these terms were found from Atomic Energy Levels and Atomic Energy Levels and Grotrian Diagrams I.[8] The Q-value into which capture may occur will yield a corresponding energy level from Equation (7b). A list of all the plotted energy levels for each spectrum is given in Table 1.

Figure 6: Partial energy-level diagram for the Ne^{+3} + He system.

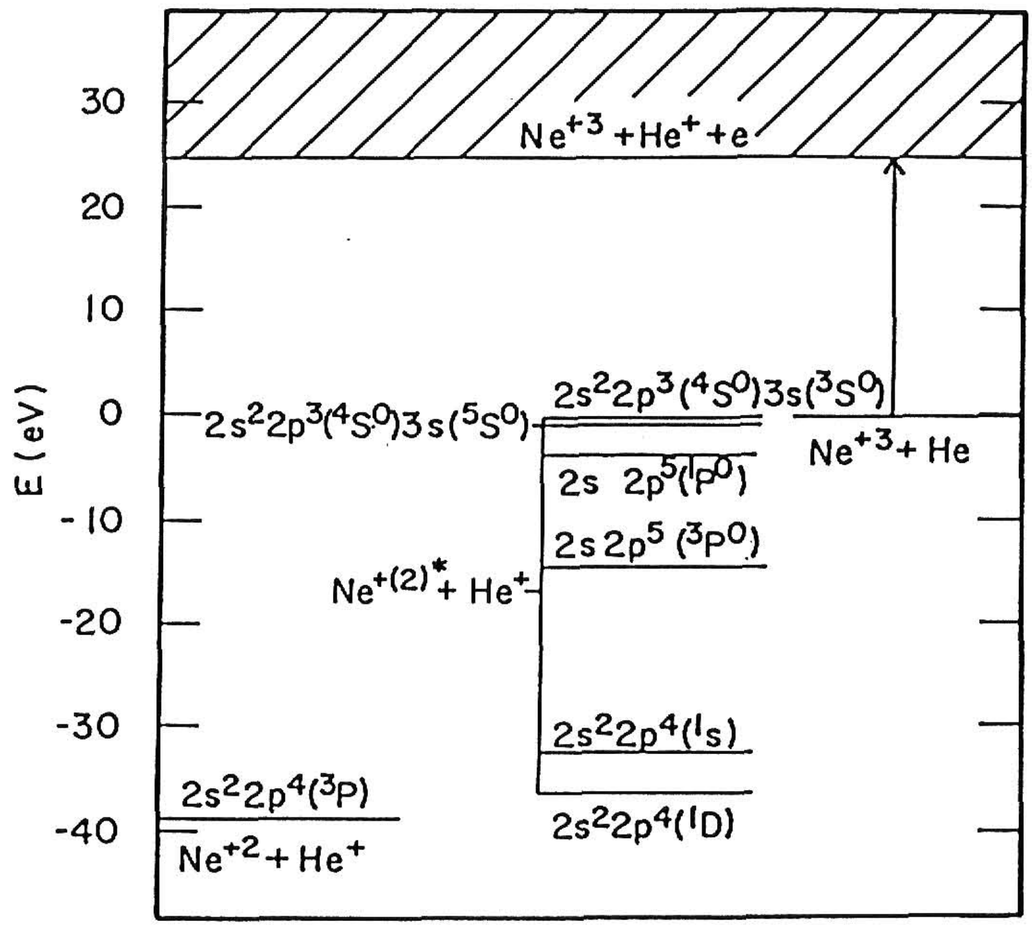

30
20
10
0
-10
-20
-30
-40
E (eV)
Ne+3 + He+ + e
2s22p3(4S0)3s(5S0)
2s22p3(4S0)3s(3S0)
Ne+3 + He
2s 2p5(1P0)
2s 2p5 (3P0)
Ne+(2)* + He+
2s22p4(1s)
2s22p4(3P)
2s22p4(1D)
Ne+2 + He+

Table 1: Q-values and configurations for charge transfer for Ne^{+q} + He system.

Table 1

System	Q(eV)	Configuration[a]
Core		
Ne^{+3} + He		
$2s^22p^3(^2P)$	36.3	$2s^22p^4(^1D)$
	32.6	$2s^22p^4(^1S)$
	14.1*	$2s2p^5(^3P^o)$
	3.6*	$2s2p^5(^1P^o)$
	0.6*	$2s^22p^3(^4S^o)3s(^5S^o)$
	-0.1*	$2s^22p^3(^4S^o)3s(^3S^o)$
Ne^{+4} + He		
$2s^22p^2(^3P)$	64.8	$2s^22p^3(^2P^o)$
	35.4*	$2s2p^4(^2S)$
	13.1	$3s(^4P)$
	11.9	$3s(^2P)$
	9.1*	$2s^22p^2(^1D)3s(^2D)$
	7.5	$3p(^4P^o)$
	6.4	$3p(^4S^o)$
	4.1*	$2s^22p^2(^1S)3s(^2S)$
	3.7*	$2s^22p^2(^1D)3p(^2F^o)$
	3.0	$3p(^2D^o)$
Ne^{+5} + He		
$2s^22p(^2P^o)$	27.7	$3s(^3P^o)$
	26.6	$3s(^1P^o)$
	22.8	$3p(^1P)$
	22.2	$3p(^3D)$
	21.4	$3p(^3S)$
	20.9	$3p(^3P)$
	19.4	$3p(^1D)$
	17.5	$3p(^1S)$

System	Q(eV)	Configuration[a]
Core		
	16.1	$3d(^3F^o)$
	16.0	$3d(^1D^o)$
	15.0	$3d(^3D^o)$
	14.6	$3d(^3P^o)$
	14.5	$3d(^1P^o)$
	13.6	$3d(^1F^o)$
	3.0	$4s(^3P^o)$
	1.8	$4s(^1P^o)$
Ne^{+6} + He		
$2s^2(^1S)$	43.8	$3s(^2S)$
	38.7	$3p(^2P^o)$
	32.1	$3d(^2D)$
	29.9*	$2s2p(^3P^o)3s(^4P^o)$
	24.4*	$2s2p(^3P^o)3p(^2P)$
	21.7*	$2s2p(^3P^o)3p(^2S)$
	21.0*	$2s2p(^3P^o)3p(^2D)$
	18.7*	$2s2p(^3P^o)3d(^4D^o)$
	17.8*	$2s2p(^3P^o)3d(^4P^o)$
	16.8*	$2s2p(^1P^o)3s(^2P^o)$
	16.0*	$2s2p(^1P^o)3d(^2F^o)$
	9.3	$4s(^2S)$
	6.8	$4p(^2P)$
	5.7	$4d(^2D)$
Ne^{+7} + He		
$2s(^2S)$	61.4	$3s(^3S)$
	58.9	$3s(^1S)$
	55.5	$3p(^1P)$

System	Q(eV)	Configuration[a]
Core		
	55.2	$3p(^3P^o)$
	52.0	$3d(^3D)$
	49.8	$3d(^1D)$
	38.1*	$2p(^2P^o)3p(^3S)$
	33.8*	$2p(^2P^o)3d(^3P^o)$
	21.6	$4s(^3S)$
	20.7	$4s(^1S)$
	19.8	$4p(^3P)$
	19.0	$4p(^1P)$
	18.0	$4d(^3D)$
	17.3	$4d(^1D)$
	4.6	$5s(^3S)$
	3.6	$5p(^1P)$
	2.1	$5d(^1D)$
	68.6	(3,3)TI
	40.6	(3,4)TI
Ne^{+8} + He		
$1s^2(^1S)$	78.1	$3s(^2S)$
	73.8	$3p(^2P^o)$
	72.2	$3d(^2D)$
	32.3	$4s(^2S)$
	30.5	$4p(^2P^o)$
	29.8	$4d(^2D)$
	11.5	$5s(^2S)$
	10.3	$5p(^2P^o)$
	10.2	$5d(^2D)$
	0.4	$6s(^2S)$

System	Q(eV)	Configuration[a]
Core		
	-0.01	$6p(^2P^o)$
	-0.4	$6d(^2S)$
	113	(3,3)TI
	75	(3,4)TI
	29	(4,4)TI
Ne^{+9} + He		
$1s(^1S)$	52.2	$4s(^3S)$
	50.1	$4s(^1S)$
	45.7	$4p(^3P^o)$
	45.2	$4f(^1F)$
	44.2	$4p(^1P^o)$
	44.1	$4d(^3D)$
	44.2	$4f(^3F^o)$
	20.4	$5f(^1F^o)$
	20.2	$5p(^3P^o)$
	19.6	$5d(^3D^o)$
	19.5	$5p(^1P^o)$
	19.4	$5f(^3F^o)$
	6.9	$6f(^1F^o)$
	6.7	$6p(^3P^o)$
	6.6	$6p(^1P^o)$
	5.9	$6f(^3F^o)$
	5.8	$6d(^3D)$
	53	(4,4)TI
	29	(4,5)TI
	5	(5,5)TI

System	Q(eV)	Configuration[a]
Core		
Ne^{+10} + He		
	60.5	$4\ell(^2L)$
	29.9	$5\ell(^2L)$
	13.2	$6\ell(^2L)$
	55	(4,5)TI
	26	(5,5)TI

[a] Omitted configuration refers to ground core state

* Indicates core excited state

Underlined configuration indicates kinematic line is shown for that state in figures 9-15.

Chapter III

RESULTS

Single capture energy-gain spectra for Ne^{+q} (q=3-10) are presented in Figures 9 through 15. These figures, for charge states +3 to +8 show energy-gain spectra at various collision energies ranging from approximately 520·eV q to 70 eV·q. The effective collision energy for each spectrum is given by $V_{acc}\cdot q$. Also shown horizontally in each spectrum are Q-values for each system labeled in terms of their energy levels. A small background was subtracted for each spectrum.

Due to low projectile velocities, kinematic effects can become substantial. Therefore kinematic curves are plotted for several representative energy levels. The energy-gain is plotted versus the scattering angle of the projectile. If the kinematic effect is large, then the cutoff of the curve is limited by the angular acceptance of the spectrometer. A dotted line is used to represent the angular acceptance cutoff.

Table 2 gives the experimental average energy released for single capture in each case, ΔE, the corresponding experimental crossing radius $R_e(\equiv(q-1)e^2/\Delta E)$, the absorbing sphere radius R_{AS}, classical barrier radius $R_{CL}(\equiv(q-1)e^2/\Delta E(n))$, where n is the principal quantum number parameter of the populated level, given by

$$n = \left[\frac{Z^2}{2I_t}\left(\frac{2\sqrt{Z}+1}{Z+2\sqrt{Z}}\right)\right]^{\frac{1}{2}} \qquad (8)$$

Here Z is the electronic charge of the projectile and I_t is the ionization potential of the target and $\Delta E(n) = q^2(13.6)$ eV/n^2. The measured cross sections for single capture, σ_m and $\overline{P} = \sigma_m/\pi R_e^2$, are also given in

Table 2

Summary of Results and Related Parameters

System	ΔE(eV)	R_e(Å)	R_{AS}(Å)	R_{CL}(Å)	n	σ_m(10^{-16} cm^2)	$\bar{P}$
Ne^{+3} + He	3.62	7.96	3.45	2.59	1.85	0.6[a]	0.003
Ne^{+4} + He	11.95	3.62	3.64	2.93	2.35	11	0.27
Ne^{+5} + He	18.0	3.20	3.91	3.23	2.83	12	0.37
Ne^{+6} + He	32.12	2.24	4.15	3.45	3.28	7[a]	0.44
Ne^{+7} + He	21.60	4.00	4.36	3.67	3.72	11[a]	0.21
Ne^{+8} + He	30.53	3.30	4.78	3.89	4.15	15[a]	0.45
Ne^{+9} + He [b]	19.5	5.88	5.43	4.10	4.57	10	0.01
Ne^{+10} + He [b]	29.9	4.33	5.62	4.29	4.98	16	0.27

[a] Partial cross section corrected for double peaking from total cross section of Justiniano (reference 3).

[b] Values obtained from R. Mann et al. (reference 4).

Table 2. The spectra and cross sections for Ne^{+9} and Ne^{+10} were obtained from Cocke and Mann.[9] Cross sections for Ne^{+3} through Ne^{+8} were obtained from Justiniano.[10]

THIS BOOK WAS BOUND WITHOUT PAGE 32.

THIS IS AS RECEIVED FROM CUSTOMER.

Chapter IV

THEORY

Two theoretical models will be presented to describe electron capture of low-energy highly charged ions from a netural target. The first is a classical model which is velocity independent, and which deals with the ability of the target electron to escape the target Coulomb potential into that of the projectile. The second is a slightly velocity dependent absorbing sphere model of Olsen and Salop[11] which is based on an extension of the Landau Zener[12] treatment of non-adiabatic energy level crossings.

Two simplifying assumptions underlie both models:

(i) The projectile is treated as a structureless charged particle.

(ii) The target is treated as a one electron atom.

A. Classical Model (CLM)

This model was proposed by Ryufuku et al.,[13] Mann et al.[14,15] and Beyer et al.[16] It relies on the assumption that capture will occur if the target electron can overcome the potential barrier between the projectile and the singly ionized target (Figure 7). The potential in which the electron is transferred is simply the sum of the potentials of each charge center

$$V(x) = \frac{-Z}{x} - \frac{1}{R-x} \tag{8}$$

where x is the distance along the internuclear axis between the target and projectile. The maximum of the potential can be found by differentiation with respect to x yielding

Figure 7: Classical model for capture reaction, schematic representation.

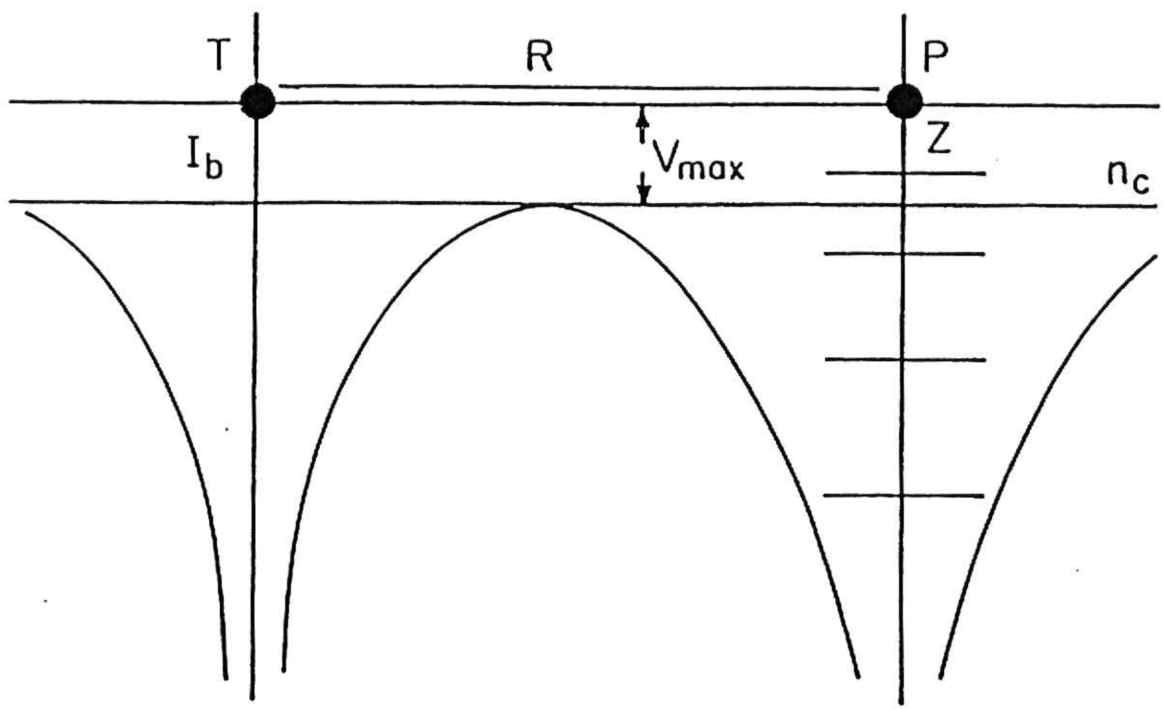
T
R
P
I_b
V_{max}
Z
n_c

$$V_{max} = \frac{-(\sqrt{Z} - 1)^2}{R} \qquad (9)$$

Two conditions must be met for capture to take place: the energy of the electron on the target must exceed the barrier maximum, and there must be a degeneracy between initial and final states (curve crossing). In the hydrogenic model of the final state, these conditions can be written as

$$-I_t - \frac{Z}{R} = \frac{-Z^2}{2n^2} - \frac{1}{R} \qquad (10a)$$

and

$$-I_t - \frac{Z}{R} \geqslant \frac{-(\sqrt{Z} - 1)^2}{R} \qquad (10b)$$

where I_t is the ionization potential of the target, n is principal quantum number of the capturing energy level, Z is the charge of the projectile and R is the distance between projectile and target. The left-hand side of Equation (10a) gives the energy of an electron bound to the target in the presence of the ionized projectiles coulomb field. The right-hand side of the equation is the energy of the electron bound to a hydrogen like level of the projectile in the presence of the potential of the ionized target. Eliminating R from Equations (10a) and (10b) and solving for n gives

$$n \leqslant \left\{\frac{Z^2}{2I_t} \left(\frac{2\sqrt{Z} + 1}{Z + 2\sqrt{Z}}\right)\right\}^{\frac{1}{2}} \qquad (11)$$

Equation (11) will not in general yield an integer value for n. Thus an integer n_c is defined as the larget integer smaller than n. Using n_c in Equation (10a) and solving for R will give the radius for capture R_c as

$$R_c = \frac{2(Z - 1)}{\frac{Z^2}{n_c^2} - 2I_t} \qquad (12)$$

Assuming the probability for capture to be ½, the electron capture cross section is given by

$$\sigma_{CLM} = \frac{\pi}{2} R_c^2 \; . \tag{13}$$

Thus the classical model predicts capture to be independent of velocity.

B. Olson and Salop Absorbing Sphere Model (OSAS)

The basic idea of the OSAS model can be presented in terms of the Landau-Zener method[18] for determining cross sections in the projectile velocity range less than 10^6 cm/s. Potential energy curves for the system $A^{+q} + B \rightarrow A^{+(q-1)*} + B^+$ are shown in Figure 8a. The Landau-Zener transition probability that the colliding particles will remain on the $A^{+q} + B$ potential curve at a curve crossing is given by

$$p = e^{-\gamma} \tag{11a}$$

$$\gamma = 2\pi \, H_{12}^2/\Delta F \, V_{rad} \tag{11b}$$

where H_{12} is one half the adiabatic spitting at the curve crossing R_x, ΔF is the difference in slopes of the adiabatic potential energy curves at R_x shown in Figure 8b, and V_{rad} is the radial velocity at the crossing distance R_x. For large values of R, H_{12} will be small and the collision system will behave diabatically. As R becomes smaller, H_{12} grows until behavior intermediate between diabatic and adiabatic occurs at the crossing. Since the capture region is crossed twice, once going in and once going out, the probability P that capture will occur is related to p by $P = 2p(1-p)$.

For a two level crossing system (one exit channel) the probability P maximizes at a value of $p = 0.5$ for $\gamma = 0.693$. For the two level system

Figure 8a: Schematic representation for the potential curves of the electron transfer reaction $A^{+q} + B \rightarrow A^{+(q-1)} + B^{+}$.

Figure 8b: Schematic representation for behavior of the adiabatic potential curves near an avoided crossing.

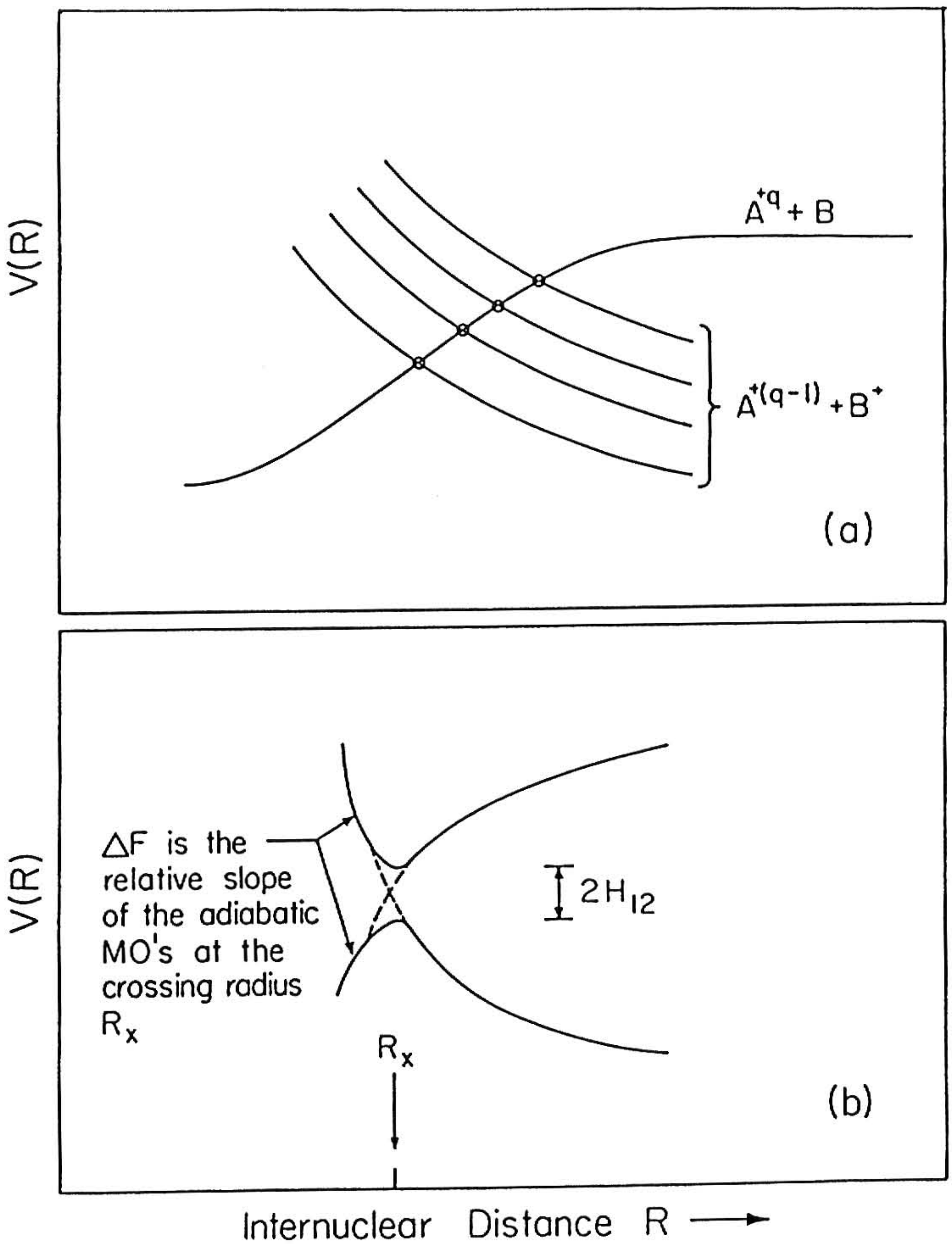
V(R)
$A^{+q} + B$
$A^{+(q-1)} + B^{+}$
(a)
V(R)
ΔF is the relative slope of the adiabatic MO's at the crossing radius R_x
$2H_{12}$
R_x
(b)
Internuclear Distance R

the matrix elements H_{12} are given by

$$H_{12}=Ae^{-BR_x} \tag{12}$$

where A and B are constants and R_x is the crossing radius. Substituting the values of γ = 0.693, $\Delta F = (q-1)/R_x^2$, $V_{rad} \approx$ incident velocity, V_o, and H_{12} from Equation (12) into Equation (11b) yields

$$R_x A^2 \exp(-2BR_x) = V_o(q-1)/2\pi \tag{13}$$

From Equation (13) the crossing radius (for a two level system) can be determined numerically.

By a similar method the crossing radii and corresponding cross sections can be found for a multi-level system. By assuming a large number of curve crossings, Olson, with a universal form for $H_{12}(R)$, has shown that an absorbing sphere model can be used. That is, inside some critical radius R_c determined by the crossing parameter the probability for capture is unity. Under the absorbing sphere assumption the cross section is given by

$$\sigma_{AS} = \pi R_c^2 \ . \tag{14}$$

An expression for the critical radius, R_c, is given by Olson and Salop as

$$0.15 = 2\pi H_{12}^2(R)/\Delta F(R)V_o \tag{15}$$

where V_o is the incident projectile velocity. The relative slope, ΔF, for the products is

$$\Delta F = (q - 1)/R^2 \ . \tag{16}$$

Olson and Salop empircally determined the coupling matrix H_{12} as

$$H_{12}^{OSAS} = \frac{9.13}{\sqrt{q}} \exp(-1.324\alpha \frac{R}{\sqrt{q}}) \tag{17}$$

where α is given in terms of the target by $\alpha = \sqrt{2I_t}$.

Combining Equations (15), (16) and (17), the critical radius is given by the expression

$$R_c^2 \exp(-2.648\alpha \frac{R_c}{\sqrt{q}}) = 2.864 \times 10^{-4}\ q(q-1)V_o \qquad (18)$$

which is dependent only upon I_t, q and incident projectile velocity. Solving Equation (18) for R_c locates the "favored radius" for capture. Substituting R_c into Equation (14) gives the corresponding cross section.

Chapter V

DISCUSSION OF RESULTS

Ne^{+3}

The energy-gain spectra for Ne^{+3} with a projectile energy of 224.07 eV·q is shown in Figure 9A. This system has three discrete energy levels lying in the favored region for capture. From Figure 9A we see population occurs at 3.62 eV and 14.11 eV. Both of these are core exicted states with configurations $1s^2 2s2p^5(^1P^o)$ and $1s^2 2s2p^5(^3P^o)$ respectively. The calculated absorbing sphere radius R_{AS} = 3.45 Å falls directly in between the experimental radii of the two populated levels at 7.96 and 2.04 Å. Figures 16-23 show partial energy-level diagrams plotted as a function V(R) versus the internuclear distance R.

The capture cross section was found to be 0.55×10^{-16} cm^2 for the 3.62 eV energy level. This cross section was adjusted by multiplying

$$\frac{\text{(area of 3.62eV peak)}}{\text{(area of 3.62 and 14.11eV peak)}} \qquad (19)$$

times the single capture cross section of Justiniano.[20] This cross section is much less than the absorbing sphere cross section given by $\sigma_{AS}=\pi R_{AS}^2=$ 37.5×10^{-16} cm^2. We attribute this to the very small coupling matrix element, H_{12}, which couples the incident channel with these core excited states. To better separate the transition probability from geometrical effects, we define a parameter $\overline{P}=\sigma_m/\pi R_e^2$ which is the ratio of the measured cross section (σ_m) to the geometrical cross section calculated from the experimental crossing radius R_e. Using the 3.62 eV energy level results in a value for

Figure 9a-b: Energy-gain spectra for the Ne^{+3} + He system at various acceleration voltages.

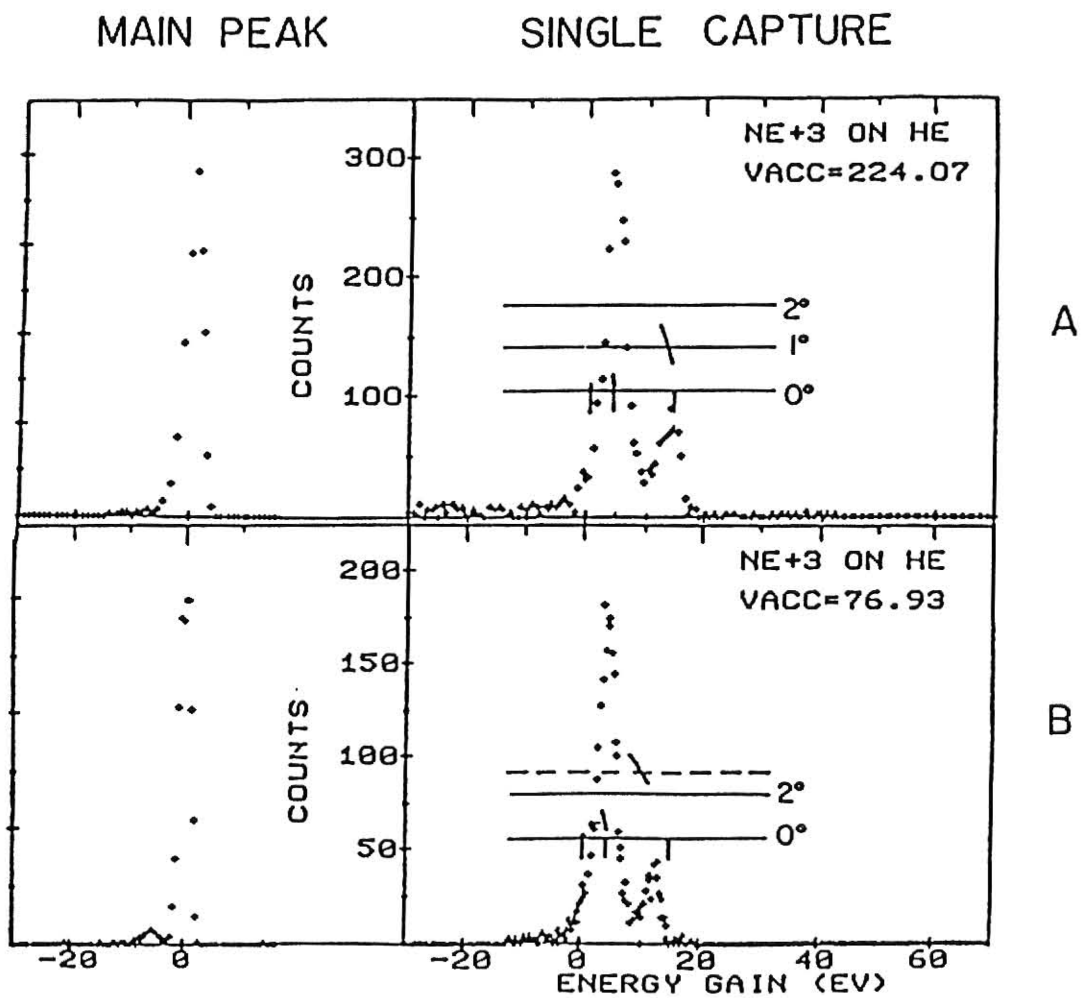

MAIN PEAK
SINGLE CAPTURE
NE+3 ON HE
VACC=224.07
300
200
100
COUNTS
2°
1°
0°
A
NE+3 ON HE
VACC=76.93
200
150
100
50
COUNTS
2°
0°
B
-20
0
-20
0
20
40
60
ENERGY GAIN (EV)

R_e of 7.96 Å, yielding a $\overline{P}$ of 0.003. The low values of $\overline{P}$ can be attributed to weak coupling to the levels which lie in the favored region, which are core excited states. Thus we can conclude that as the projectile approaches the target the probability for capture increases until it maximizes near R_{AS}. However, due to the non-continuum of energy levels the projectile is forced to capture at the nearest available curve crossing.

The kinematic spread and shift (in Figure 9A and B) for the $^1P^o$ core excited state is small due to its small Q-value and the high projectile energy. However, the peak corresponding to population of the 14.11 eV level has both a greater spread and shift, thus causing the peak to appear somewhat skewed. Figure 9B shows the spectrum for a projectile energy of 76.93 eV·q. The populated levels remain the same, but the spread and shift of the 14.11 eV peak is much greater. In this case the angular acceptance of the spectrometer (2.8°) truncates drastically events from capture to this level.

Ne^{+4}

Figures 10A through 10D show energy-gain spectra for Ne^{+4} with projectile energies of 523.53 to 72.09 eV·q. The n=3 energy levels have now become open to population. There are 5 known states, based on the ^3P ground state projectile core, available to be populated in the favored region, two 3s and three 3p states. At 523.53 eV·q the 3s levels are populated. These states have energies of 13.13 and 11.95 eV with core configurations $1s^2 2s^2 2p^2(3S)$ yielding (^4P) and (^2P) states respectively. The two populated states correspond to experimental crossing radii, R_e, of 3.29 and 3.62 Å. The absorbing sphere radius R_{AS}=3.64 Å compares well with the experimental radii. The 3p levels are apparently not populated because their crossing radii are significantly greater than R_{AS}. There is no evi-

Figure 10a-d: Energy-gain spectra for the Ne^{+4} + He system at various acceleration voltages.

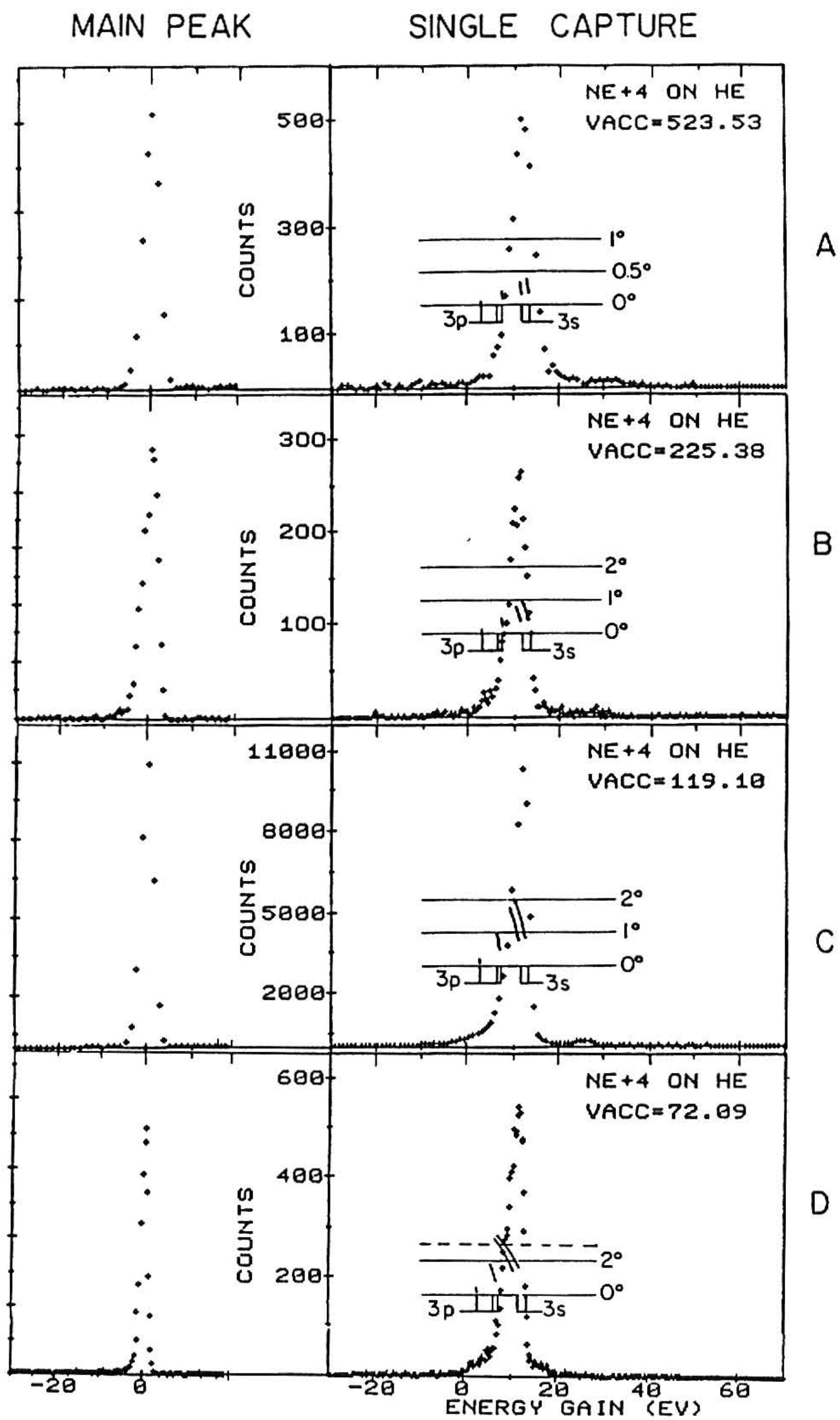
MAIN PEAK
SINGLE CAPTURE
NE+4 ON HE
VACC=523.53
NE+4 ON HE
VACC=225.38
NE+4 ON HE
VACC=119.10
NE+4 ON HE
VACC=72.09
COUNTS
ENERGY GAIN (EV)
3p
3s
0°
0.5°
1°
2°
A
B
C
D

dence that the ^2D state at 9.1 eV is being populated. This is especially apparent at lower energies, where kinematic shifts at 72.09 and 119.1 eV·q are large so that the 3s level at 9.12 eV should be apparent if it were populated.

The measured cross section for Ne^{+4} given by Justiniano is $\sigma_m = 11 \times 10^{-16}$ cm^2. Using the crossing radius of 3.62 Å yields a value of $\overline{P}$ of 0.27.

Evidence for the 2.8° angular cutoff is seen in Figure 10D.

<u>Ne^{+5}</u>

Energy-gain spectra for Ne^{+5} are shown in Figures 11A through 11C. The density of available states has increased for this system giving rise to population of the 3p and 3d energy levels. Due to the large density of states, one 3p and four 3d states (lying inside the plotted 3p and 3d groupings) are not shown in the figures (Table 1).

The experimental radius can be determined by choosing a centrally located energy among all the levels being populated. At 18 eV the experimental radius is 3.20 Å. This value of R_e does not compare well with the absorbing sphere radius of 4.17 Å. $\overline{P}$ yields a value of 0.37.

<u>Ne^{+6}</u>

The Ne^{+6} energy-gain spectra are shown in Figures 12A through 12D. For this system only four core states (3d, 4s, 4p, 4d) are available for population. The 3d level at 32.12 eV is highly exoergic yielding a crossing radius of 2.24 Å. The n=4 levels are slightly exoergic, with the 4p level R_x=10.53 Å. The absorbing sphere radius at 522.91 eV·q is 4.15 Å which is significantly less thant the n=4 levels and greater than the 3d level. Thus no states built on the projectile core lie in the favored

Figure 11a-c: Energy-gain spectra for the Ne^{+5} + He system at various acceleration voltages.

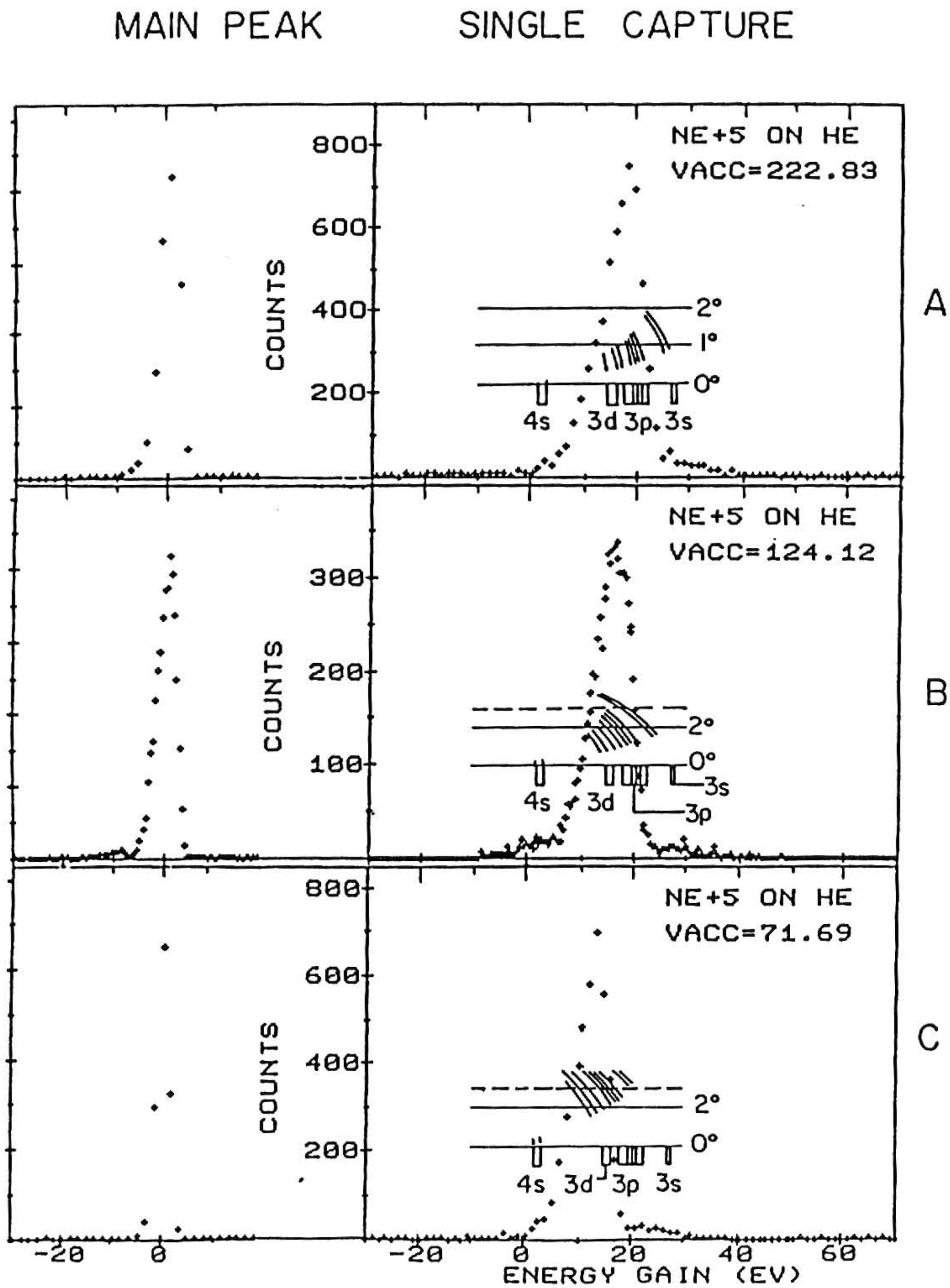

MAIN PEAK
SINGLE CAPTURE
NE+5 ON HE
VACC=222.83
NE+5 ON HE
VACC=124.12
NE+5 ON HE
VACC=71.69
COUNTS
800
600
400
200
300
200
100
2°
1°
0°
4s
3d
3p
3s
A
B
C
-20
0
20
40
60
ENERGY GAIN (EV)

Q-value region. Figure 12A shows strong population of the 3d level and population of various core excited states (Table 1). The series of spectra can be explained by the following. The maximum probability for capture occurs near the absorbing radius for a state with the projectile core lying in the favored region. However, at R_{AS} no core-based configurations are available. Thus some ions cpature into an excited configuration at R_{AS}, but a majority capture at a smaller radius at the first core configuration (3d). There are two mechanisms competing for capture in this system: (1) capture at the preferred radius, and (2) capturing to a favored configuration at 522.91 eV·q the single 3d core configuration dominates. The fact that the absorbing sphere model is velocity dependent may be seen from comparison of Figures A and B. As the projectile energy decreases we see the population of the 3d level favored by configuration, decreases relative to that of the core excited states. This could be due to the increasing value of R_{AS} as the projectile velocity decreases. The larger value of R_{AS} forces smaller Q-value states to be populated.

At 522.91 eV·q where capture into a core state is dominant the measured cross section is 7.0×10^{-16} cm^2. This cross section was adjusted by the method used for Ne^{+3}. The 3d and 21.0 eV core excited state yield values of $\overline{P}$ of 0.44 and 0.1 respectively. The small values of $\overline{P}$ for the latter case are due to the population of core excited states. The H_{12} responsible for population of such states are small, and thus will yield a measured cross section which is less than πR_e^2.

As discussed in Chapter II, Section 3, the Ne^{+6} spectra C and D show strong evidence for the 2.8^0 angular cutoff in the truncated population for the 3d level.

Figure 12a-d: Energy-gain spectra for the Ne^{+6} + He system at various acceleration voltages.

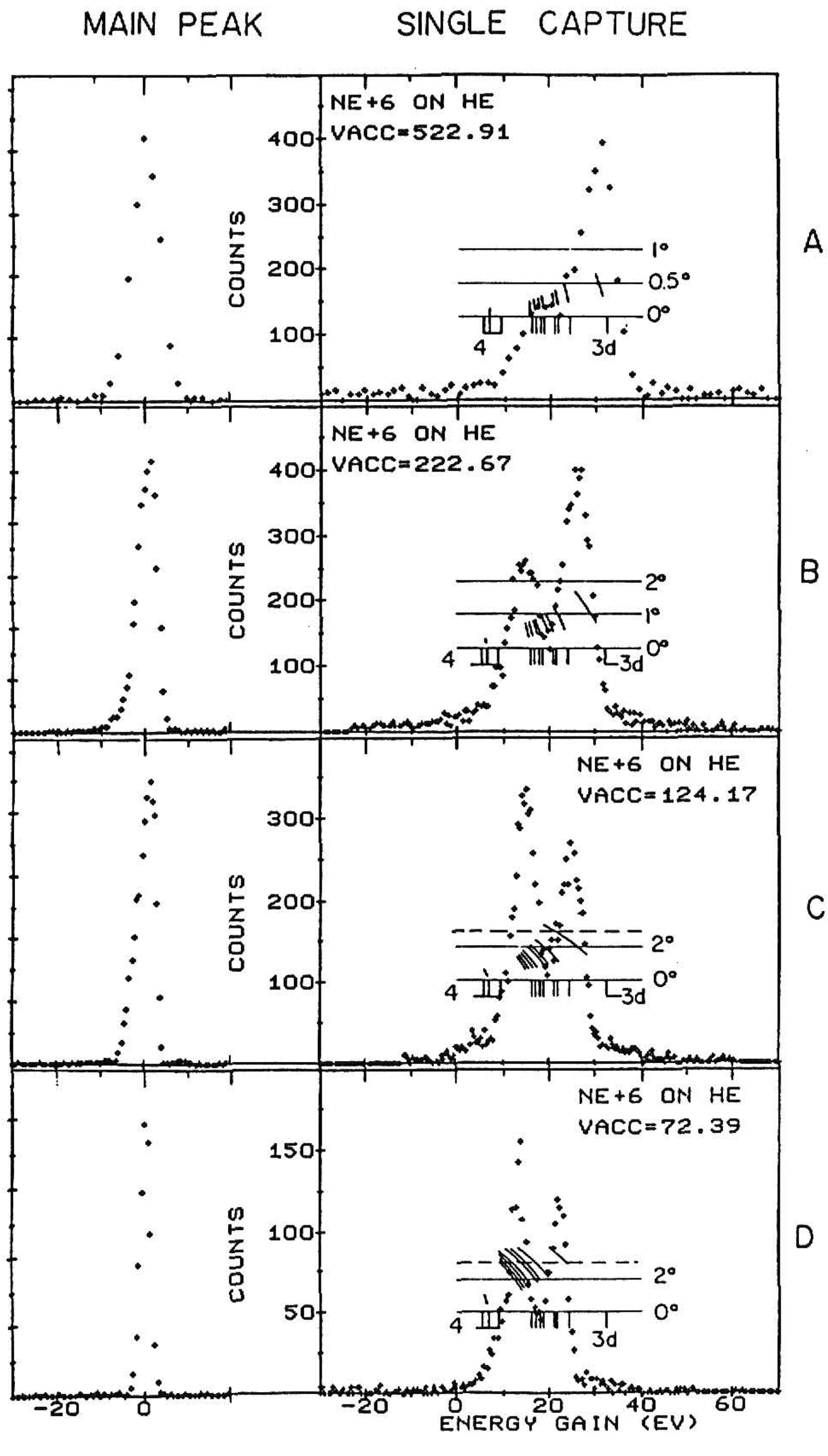
MAIN PEAK
SINGLE CAPTURE
NE+6 ON HE
VACC=522.91
A
NE+6 ON HE
VACC=222.67
B
NE+6 ON HE
VACC=124.17
C
NE+6 ON HE
VACC=72.39
D
COUNTS
ENERGY GAIN (EV)
4
3d
0°
0.5°
1°
2°

Ne^{+7}

In the Ne^{+7} spectra (shown in Figures 13A through 13D) the n=4 energy levels have now become favorable for population. There is no population of the n=3 and n=5 energy levels due to the large exoergicity of the n=3 level and only the slight exoergicity of the n=5 level. Six n=4 levels are available for capture, although only three are plotted (Table 1). Capture into a 4s level at 21.60 eV with a configuration of $1s^2 2s^2 4s(^3S)$, which appears to be favored in the spectra, yields R_e=4.00 Å. This value of R_e is slightly less than the absorbing radius of 4.36 Å. Using R_e for the n=4 capture and a modified value of the cross section (due to double peaking outlined for Ne^{+3}) $\overline{P}$ was found to be 0.21.

Small population of transfer ionization channels (3,4) TI and (3,3) TI are observed at energies near 50 eV and 70 eV respectively. Here the apparent single capture is presumed to occur through double capture of electrons into shells n and n', followed by autoionization. The notation used is (n,n') TI. The Q-values for TI were estimated using the known binding energies of relevant singly excited states. Transfer ionization of one part in seven of normal single capture has also been observed for Ne^{+7} on He at projectile energies of 500 eV/q by Justiniano.[21] As in the case of Ne^{+6} and Ne^{+7}, capture channels above the absorption radius diminish in intensity for decreasing projectile energy.

Due to the large Q-value of (3,3) TI and the n=3 levels the kinematic shifts make it difficult to distinguish n=3 from (3,3) TI. However, Figures 5A and 5B are consistent with population of states of either type.

Ne^{+8}

Energy-gain spectra for Ne^{+8} are shown in Figures 14A through 14C.

Figure 13a-d: Energy-gain spectra for the Ne^{+7} + He system at various acceleration voltages.

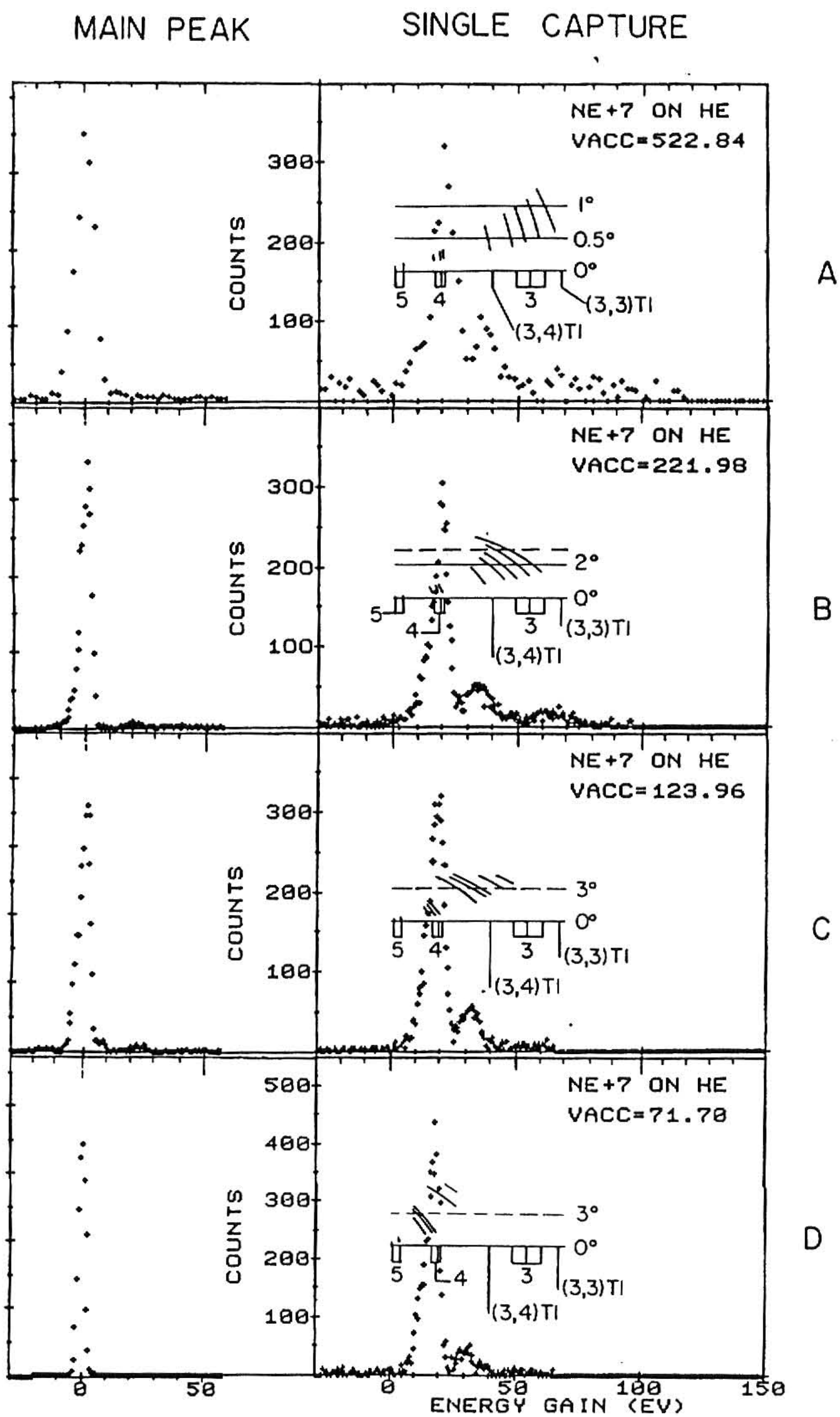

MAIN PEAK
SINGLE CAPTURE
NE+7 ON HE
VACC=522.84
NE+7 ON HE
VACC=221.98
NE+7 ON HE
VACC=123.96
NE+7 ON HE
VACC=71.70
COUNTS
ENERGY GAIN (EV)
(3,4)TI
(3,3)TI
A
B
C
D

Strong population at all projectile energies occurs for the n=4 energy levels around 30.53 eV. This corresponding to an experimental crossing radius of 3.30 Å. The absorption radius at 224.61 eV·q was found to be 4.78 Å, which would yield a Q-value of 21.10 eV. The discrepancy between R_e and R_{AS} is due to the lack of levels available for population. The n=5 energy levels lie at a crossing radius of 9.78 Å. Therefore since population will occur near or inside R_{AS} (=4.78 Å), population cannot happen until the first available states appear near 3.30 Å.

The value of $\overline{P}$ was determined using a cross section modified as in the Ne^{+3} case due to the double peaking of the spectrum. A value of $\overline{P}$=0.45 was found for the n=4 capture. A larger kinematic shift accounts for the low energy-gain of the TI peak. The approximation one-to-five ratio of transfer ionization to single capture seen in spectra 14A and B agrees well with that observed by Justiniano.

Ne^{+9}

The cases of Ne^{+9} and Ne^{+10} are included here only for completeness; the data are due to Mann et al.[22] and do not form part of the present experimental work.

Figure 15A shows the energy-gain spectrum for Ne^{+9} at a projectile energy of 49.2 eV·q. One dominant peak is seen populating the n=5 energy levels. The 19.5 eV level has a crossing radius of 5.88 Å. This result is in good agreement with the absorbing radius of 5.43 Å. A small value of $\overline{P}$ (=0.10) results since the one electron ion presents only a few energy levels (lying extremely close together) available for population near the absorption radius.

Figure 14a-b: Energy-gain spectra for the Ne^{+8} + He system at various acceleration voltages.

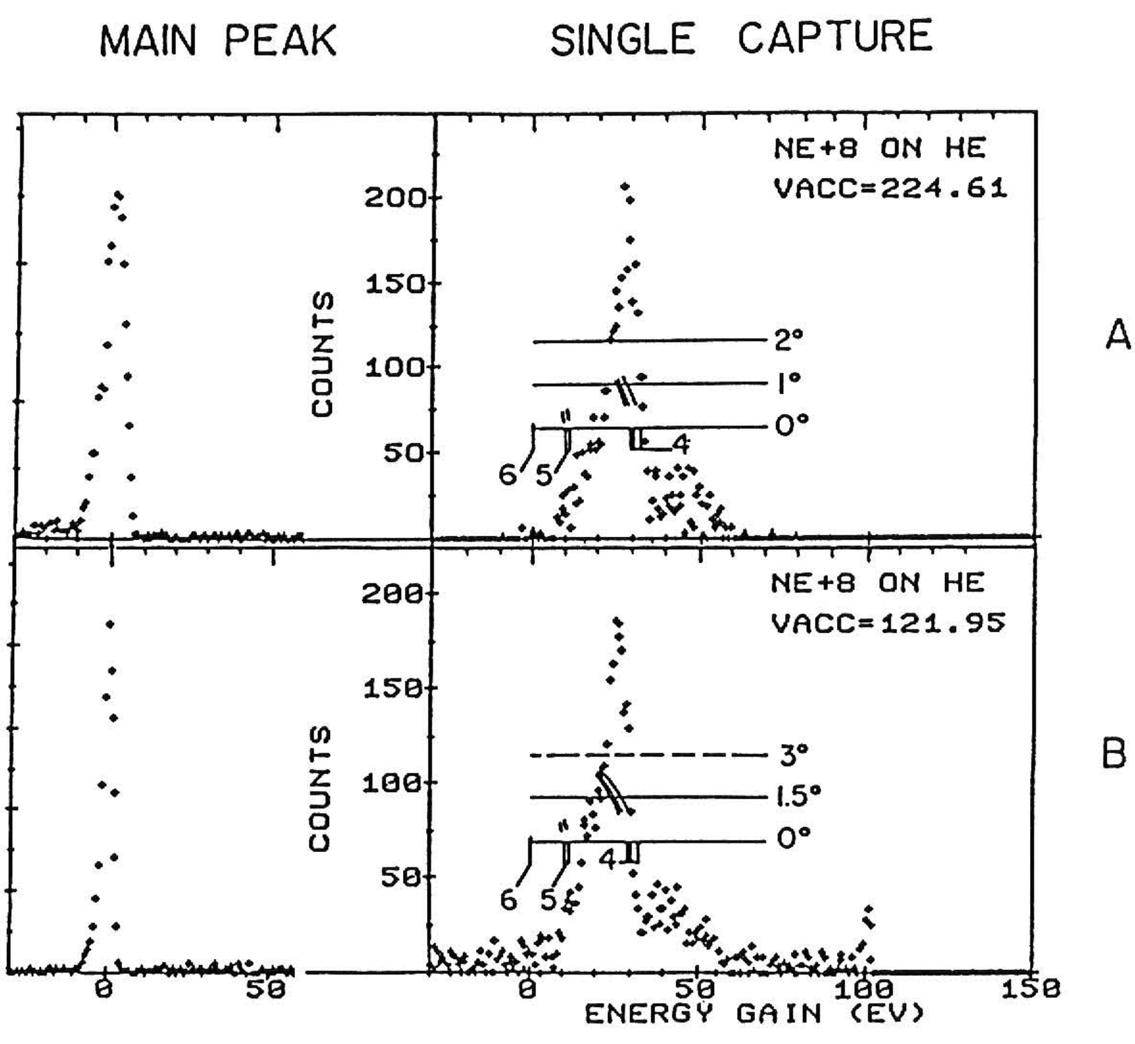
MAIN PEAK
SINGLE CAPTURE
NE+8 ON HE
VACC=224.61
200
150
100
50
COUNTS
2°
1°
0°
6
5
4
A
NE+8 ON HE
VACC=121.95
3°
1.5°
B
0
50
100
150
ENERGY GAIN (EV)

Figure 15a: Energy-gain spectra for the Ne^{+9} + He system at various acceleration voltages.

Figure 15b: Energy-gain spectra for the Ne^{+10} + He system at various acceleration voltages.

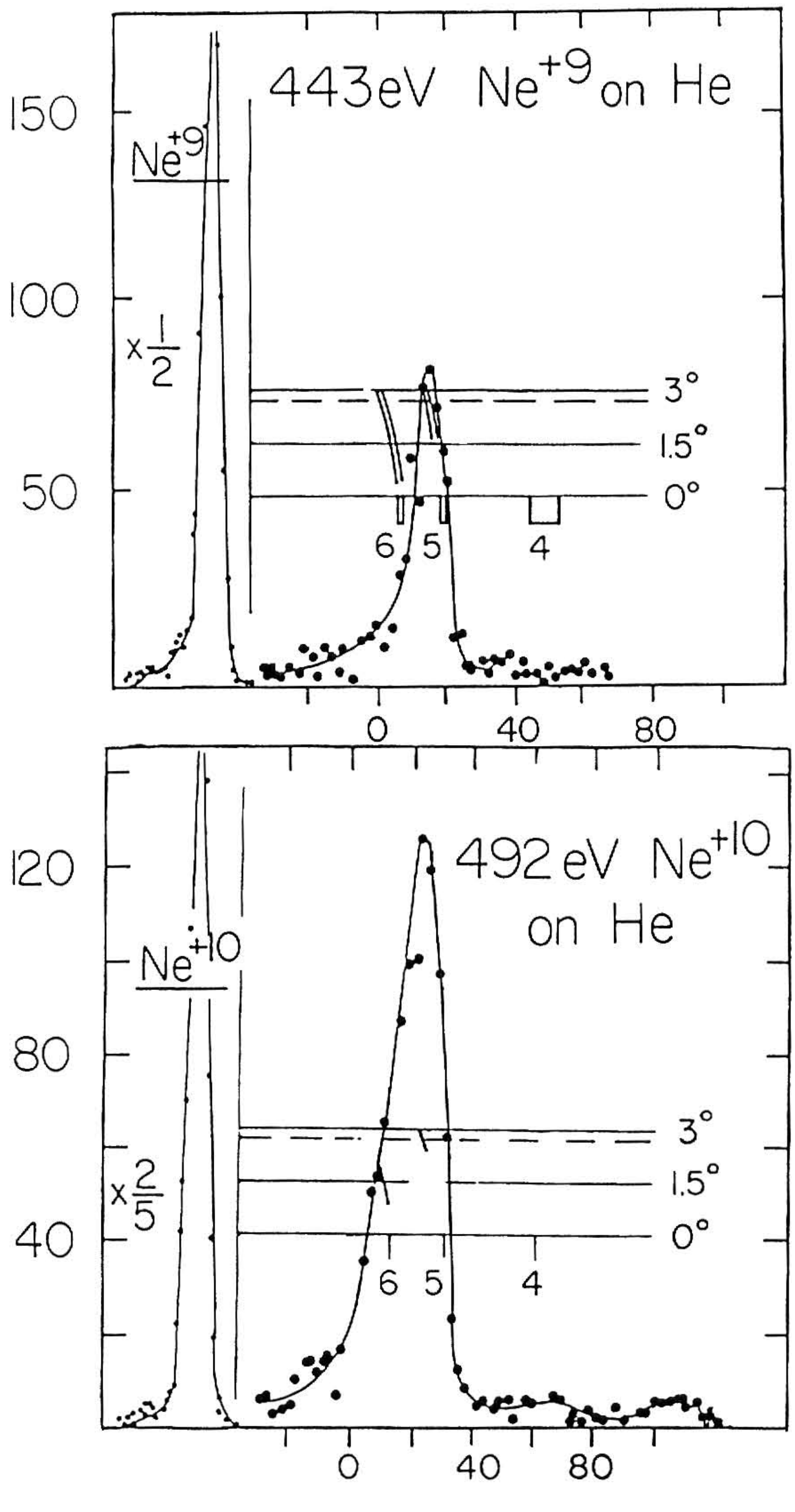
443eV Ne^{+9} on He
Ne^{+9}
$\times\frac{1}{2}$
150
100
50
3°
1.5°
0°
6
5
4
0
40
80
492 eV Ne^{+10} on He
Ne^{+10}
$\times\frac{2}{5}$
120
80
40
3°
1.5°
0°
6
5
4
0
40
80

$\underline{Ne^{+10}}$

Population of a single peak for Ne^{+10} at 49.2 eV·q is shown in Figure 15B. The hydrogen-like ion has states degenerate and unresolvable for a given n. The n=5 energy levels are being populated at a Q-value of 29.9 eV. This results in a crossing radius of 4.33 Å. This value of R_e is in good agreement with the absorbing sphere of 5.62 Å. For this case, $\overline{P}$ is found to be 0.27.

Figure 16: Partial energy-level diagram for the Ne^{+3} + He system. All levels were obtained from tables of reference 7 and 8.

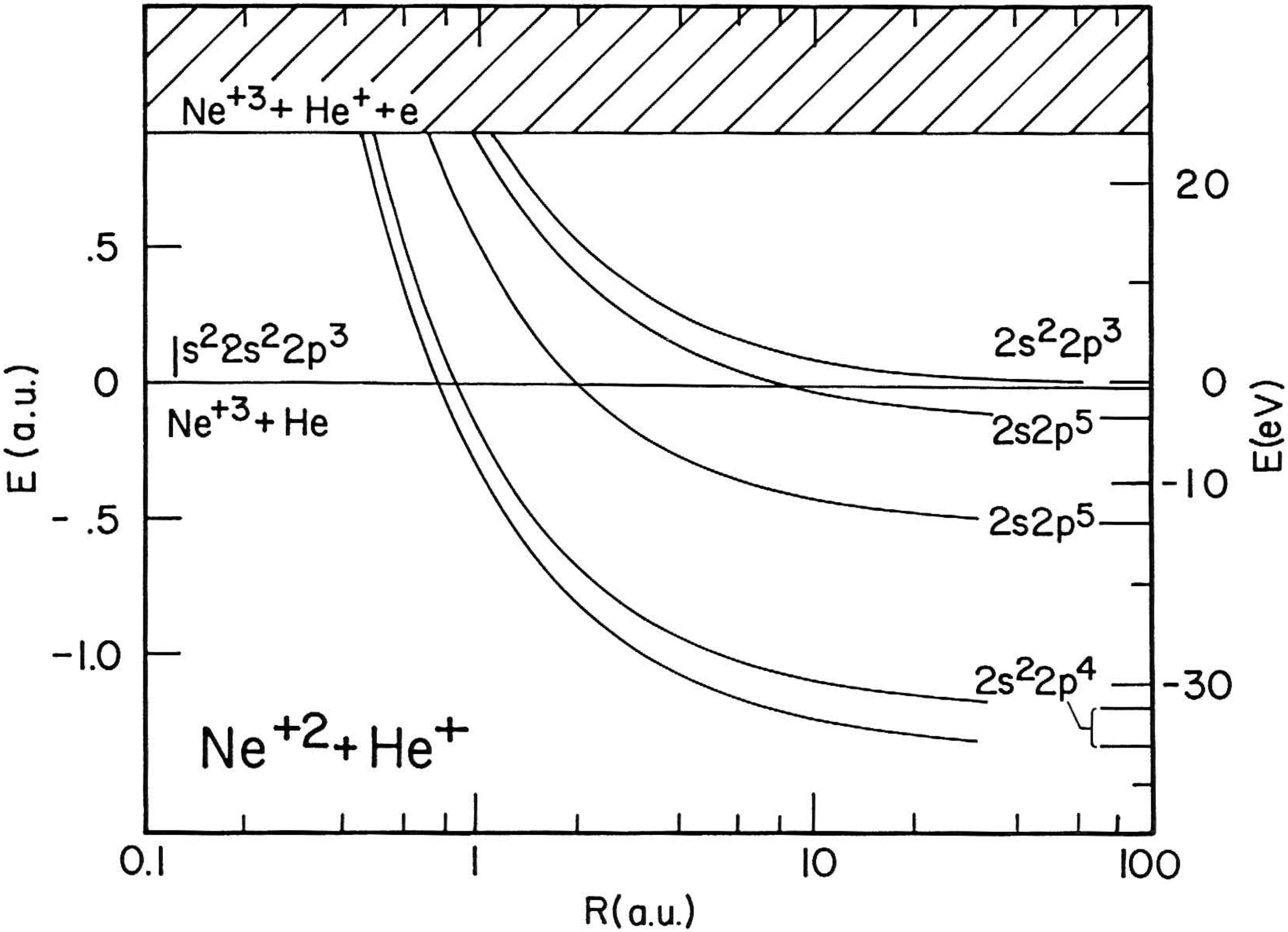

Ne+3+ He++e
1s22s22p3
Ne+3+ He
Ne+2+ He+
2s22p3
2s2p5
2s2p5
2s22p4
.5
0
- .5
-1.0
E (a.u.)
20
0
-10
-30
E(eV)
0.1
1
10
100
R(a.u.)

Figure 17: Partial energy-level diagram for the Ne^{+4} + He system. All levels were obtained from tables of reference 7 and 8.

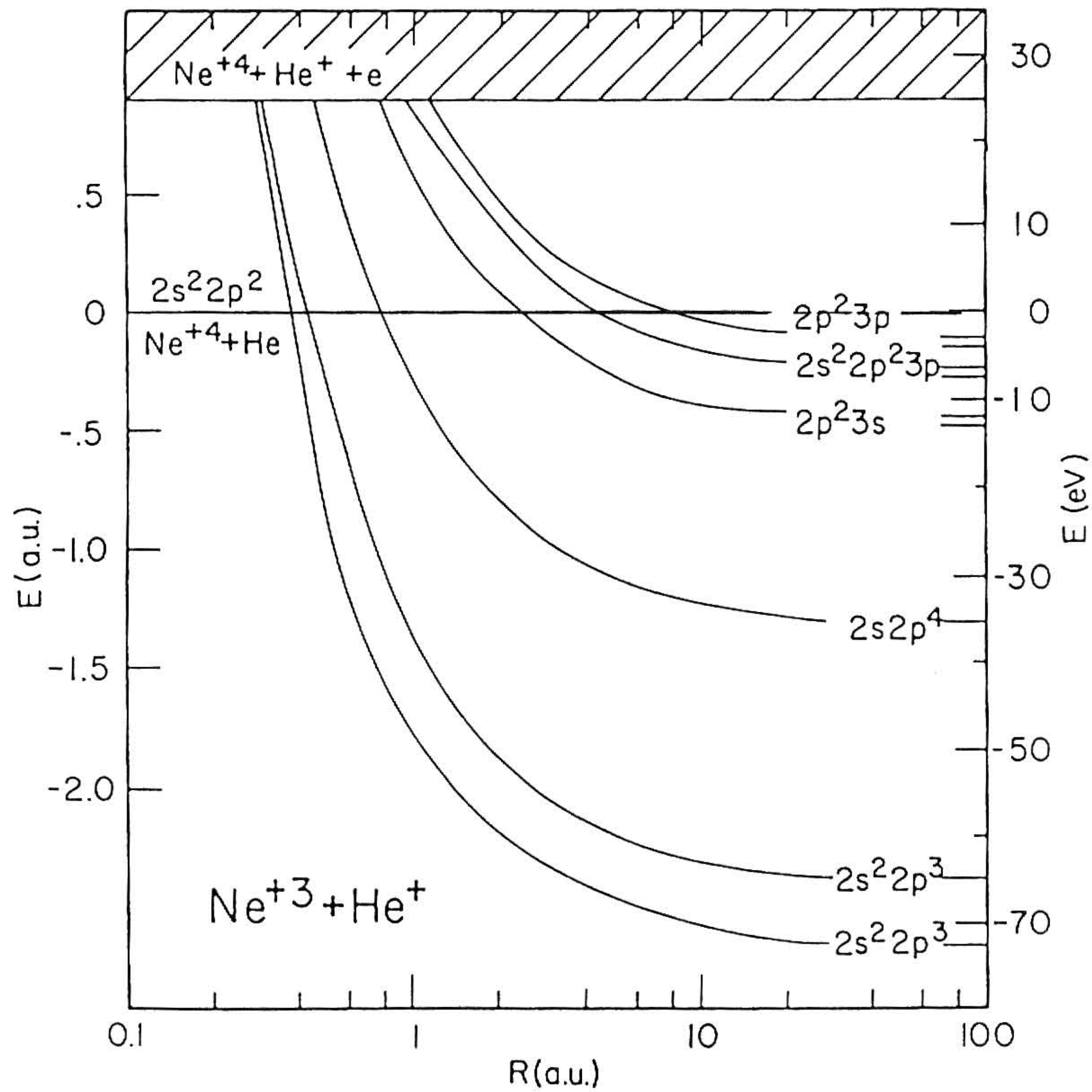

Ne^{+4}+ He^{+} +e
.5
0
-.5
-1.0
-1.5
-2.0
E (a.u.)
2s^{2}2p^2
Ne^{+4}+He
Ne^{+3}+He^{+}
2p^{2}3p
2s^{2}2p^{2}3p
2p^{2}3s
2s2p^4
2s^{2}2p^3
2s^{2}2p^3
30
10
0
-10
-30
-50
-70
E (eV)
0.1
1
10
100
R(a.u.)

17

Figure 18: Partial energy-level diagram for the Ne^{+5} + He system. All levels were obtained from tables of reference 7 and 8.

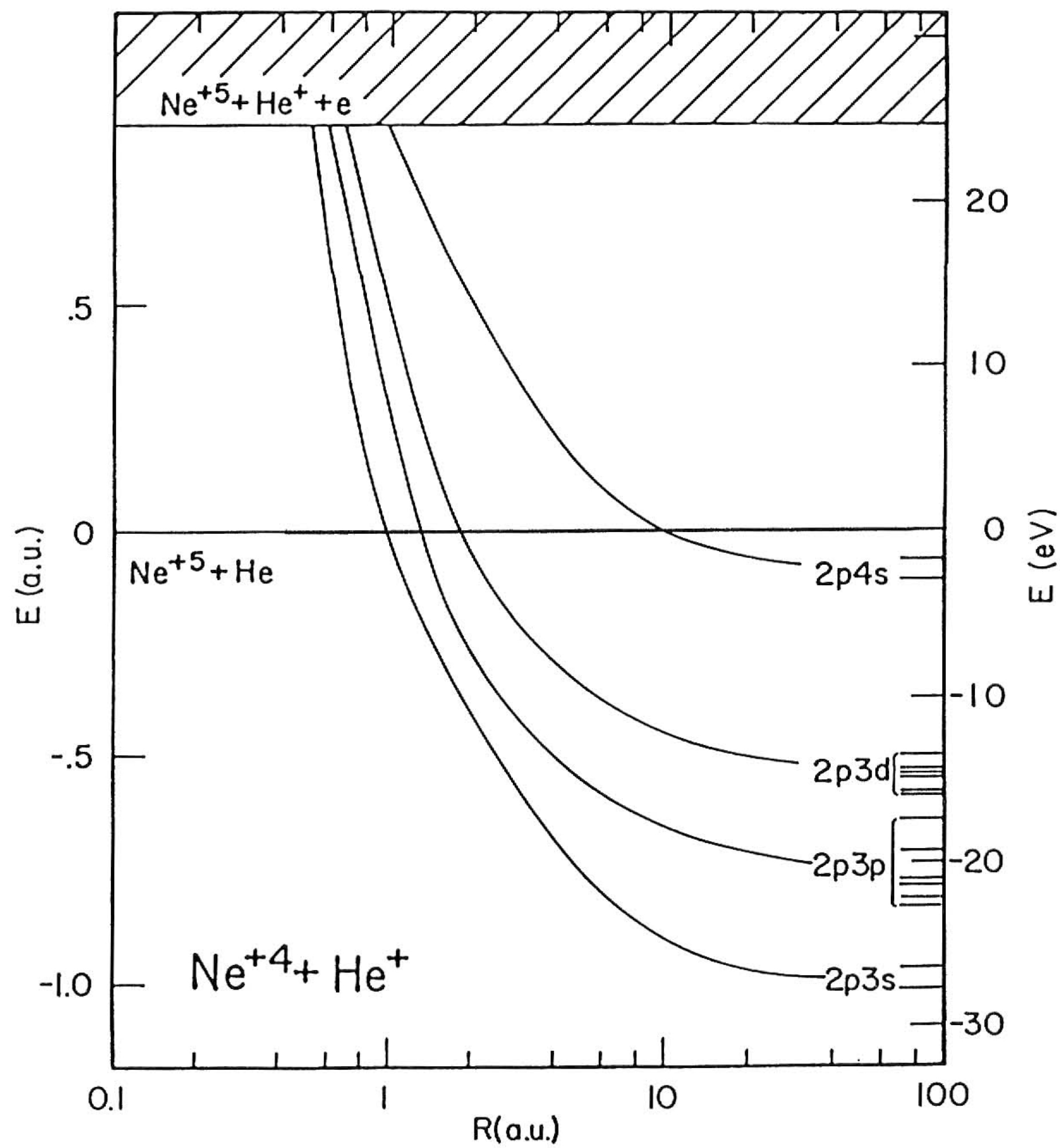
Ne+5+ He+ +e
Ne+5+ He
Ne+4+ He+
2p4s
2p3d
2p3p
2p3s
E (a.u.)
E (eV)
R(a.u.)
.5
0
-.5
-1.0
20
10
0
-10
-20
-30
0.1
1
10
100

Figure 19: Partial energy-level diagram for the Ne^{+6} + He system. All levels were obtained from tables of reference 7 and 8.

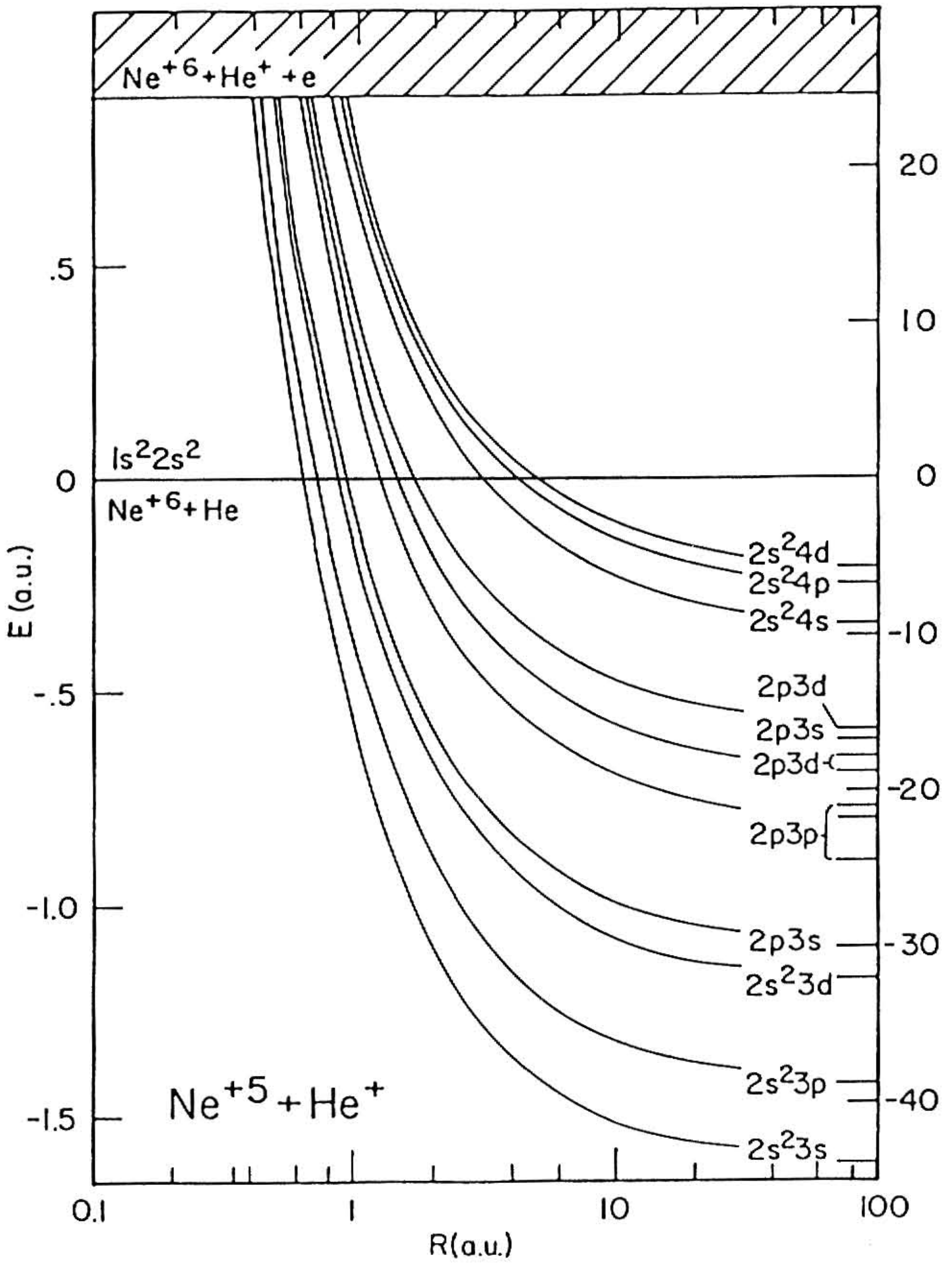
Ne^{+6}+He^{+} +e
Is^{2}2s^{2}
Ne^{+6}+ He
Ne^{+5} + He^{+}
2s^{2}4d
2s^{2}4p
2s^{2}4s
2p3d
2p3s
2p3d
2p3p
2p3s
2s^{2}3d
2s^{2}3p
2s^{2}3s
.5
0
-.5
-1.0
-1.5
E (a.u.)
20
10
0
-10
-20
-30
-40
E (eV)
0.1
1
10
100
R(a.u.)

19

Figure 20: Partial energy-level diagram for the Ne^{+7} + He system. All levels were obtained from tables of reference 7 and 8.

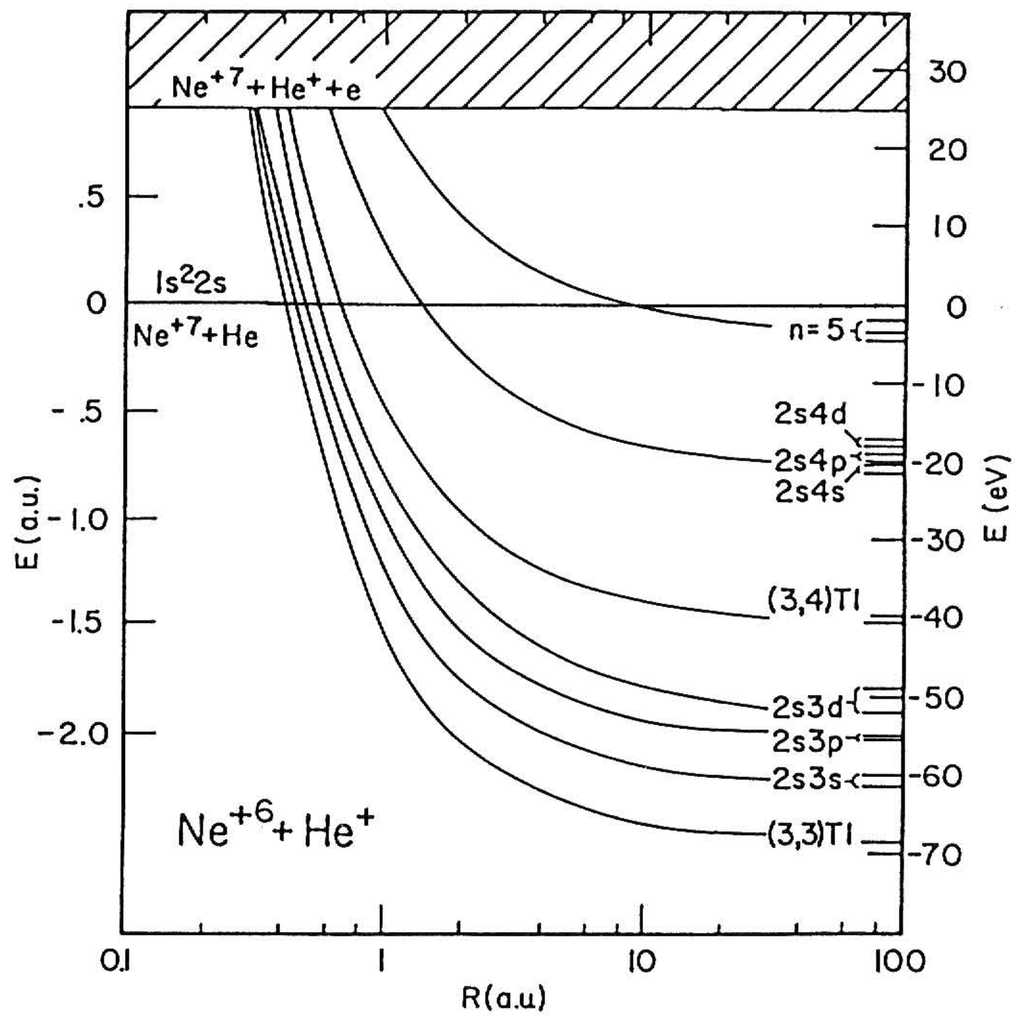
Ne^{+7}+He^{+}+e
.5
$1s^2 2s$
0
Ne^{+7}+He
-.5
-1.0
-1.5
-2.0
E (a.u.)
Ne^{+6}+ He^{+}
n=5
2s4d
2s4p
2s4s
(3,4)T1
2s3d
2s3p
2s3s
(3,3)T1
30
20
10
0
-10
-20
-30
-40
-50
-60
-70
E (eV)
0.1
1
10
100
R(a.u)

20

Figure 21: Partial energy-level diagram for the Ne^{+8} + He system. All levels were obtained from tables of reference 7 and 8.

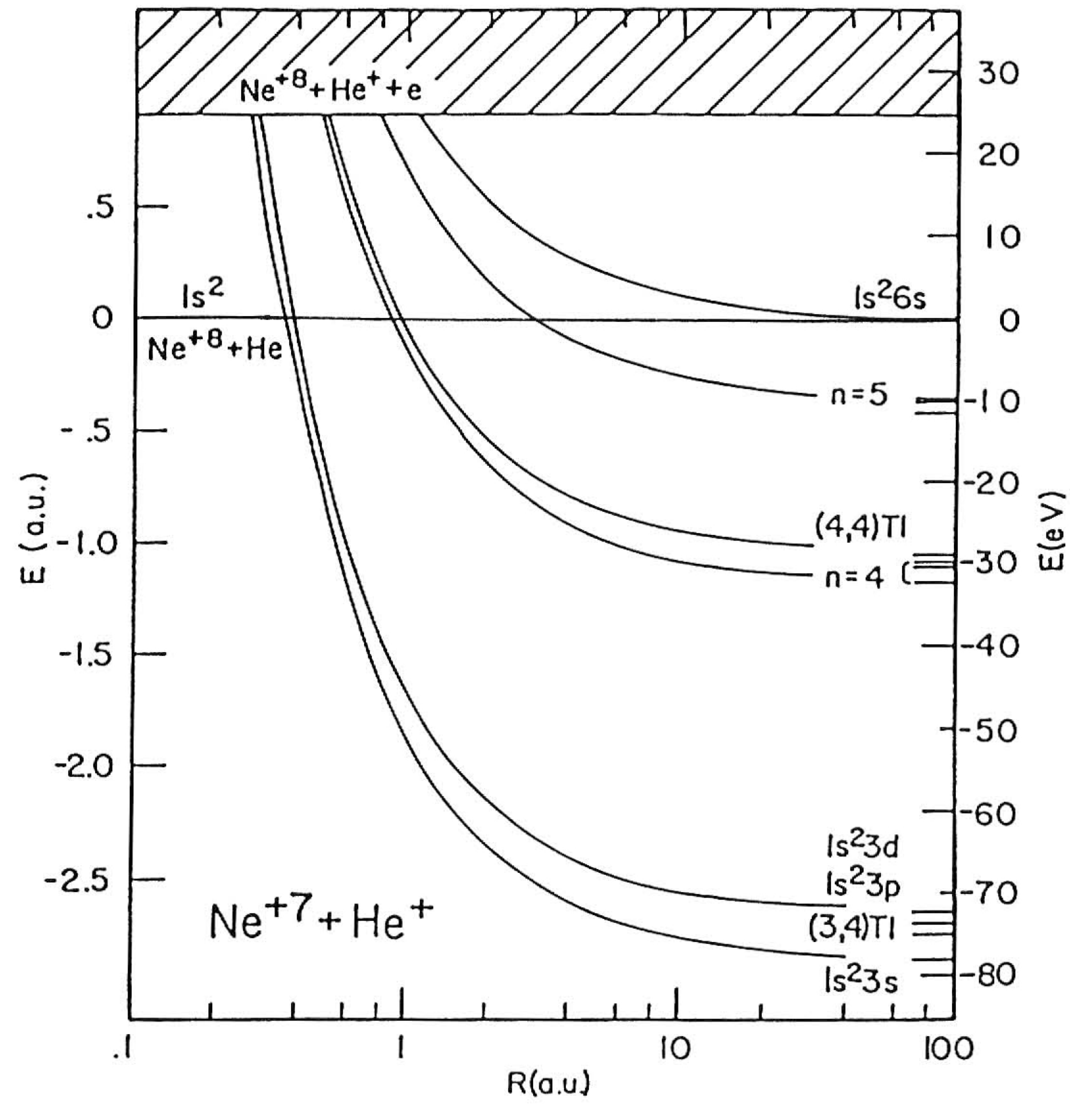
Ne+8+He++e
.5
Is2
0
Ne+8+He
- .5
E (a.u.)
-1.0
-1.5
-2.0
-2.5
Ne+7+He+
30
20
10
Is26s
0
n=5
-10
-20
(4,4)TI
n=4
-30
E(eV)
-40
-50
-60
Is23d
Is23p
-70
(3,4)TI
Is23s
-80
.1
1
10
100
R(a.u.)

Figure 22: Partial energy-level diagram for the Ne^{+9} + He system. All levels were obtained from tables of reference 7 and 8.

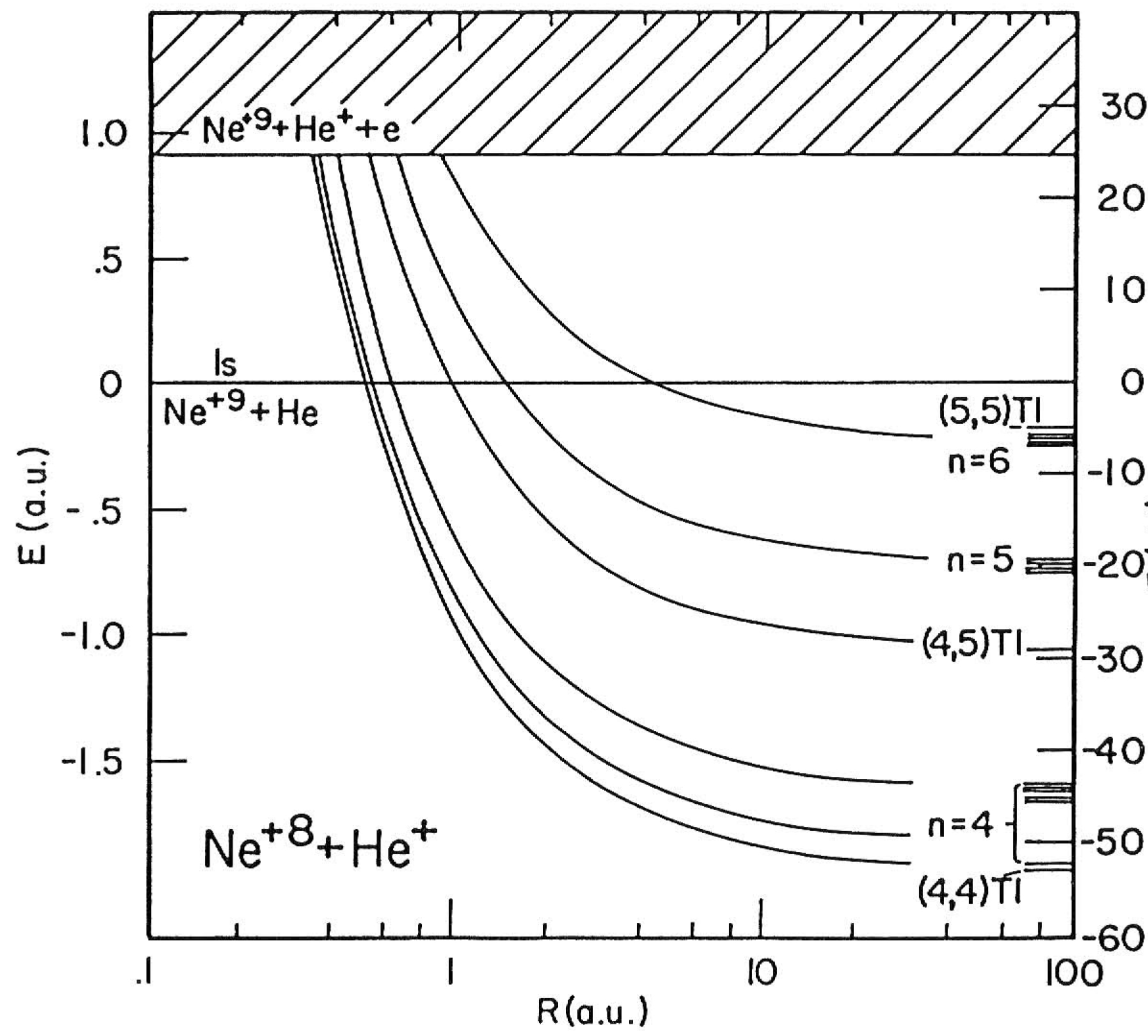

Ne+9 + He+ + e
1.0
.5
0
-.5
-1.0
-1.5
E (a.u.)
1s
Ne+9 + He
Ne+8 + He+
(5,5)TI
n=6
n=5
(4,5)TI
n=4
(4,4)TI
30
20
10
0
-10
-20
-30
-40
-50
-60
E (eV)
.1
1
10
100
R (a.u.)

Figure 23: Partial energy-level diagram for the Ne^{+10} + He system. All levels were obtained from tables of reference 7 and 8.

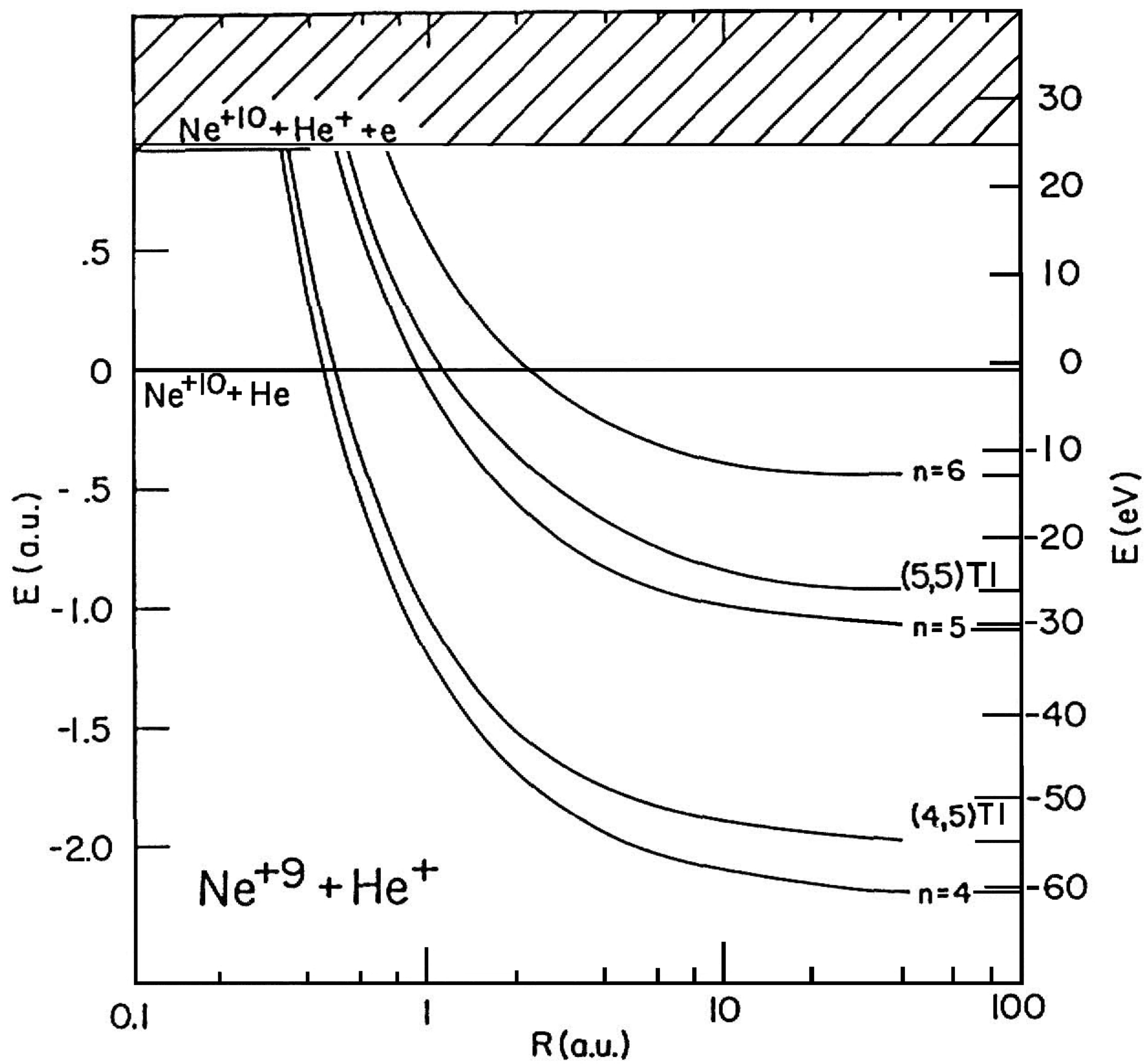

Ne+10 + He+ + e
.5
0
Ne+10 + He
- .5
-1.0
-1.5
-2.0
E (a.u.)
Ne+9 + He+
n=6
(5,5)TI
n=5
(4,5)TI
n=4
30
20
10
0
-10
-20
-30
-40
-50
-60
E (eV)
0.1
1
10
100
R (a.u.)

Chapter VI

CONCLUSIONS

Energy-gain spectra for the system N^{+q} (q=3-10) on helium were measured for low energy highly charged projectile ions having energies 50 eV·q to 520 eV/q. The projectile velocities were low (10^6 - 10^7 cm/s) compared to the velocities of the target electrons. Fast pulsed heavy ion beams produced by a tandem Van de Graaff accelerator were used to produce the source of low-energy highly charged projectiles.

The presented classical model is able to correctly predict the populated n-values for each system. This velocity independent model fails to correctly predict the crossing radius and corresponding cross section. The general features of each spectrum can be explained well with the Olsen and Salop absorbing sphere (OSAS) model. The model states states the probability of capture will be unity inside a sphere of radius R_{AS}. This is true provided a continuum or high density of states exist near R_{AS}. However for our non-idealized system we can assume capture will occur at or inside the absorption radius depending upon the availability of states. Evidence of this is seen in all the energy-gain spectra from the fact that the experimental crossing radius nearly agrees with the absorption radius. The favored energy levels to which capture may occur are independent of n or ℓ values and are determined strictly by the availability of states near the absorption radius. Strong evidence of this is seen in the Ne^{+3} and Ne^{+6} spectra where population of core excited states dominates over ground core states in an effort to capture at the desired absorption radius. The small cross sections can be attributed to population of core excited states. The small cross sections yield a reduced value of $\overline{P}$. The reduced cross sections can be explained by the small value of the coupling matrix H_{12} due to the population of the core excited states.

Small values of $\overline{P}$ can also be attributed to capturing at radii other than the absorption radius. Deviations from the absorbing sphere radius is contributed largely to the non-continuum of levels available for population. It can be concluded that the OSAS model predicts the systematics of the capture process quite well. The capture process for the Ne^{+q} + He system is strongly governed by the absorption radius and is independent of the n or ℓ value.

REFERENCES

1. D. M. Meade, Nucl. Fusion 14, 289 (1974).
2. H. Vermichel and J. Bodhansky, Nucl. Fusion 18, 1467 (1978).
3. E. Justiniano, Ph.D. Dissertation (Kansas State University, 1982).
4. R. Mann, C. L. Cocke, A. S. Schlachter, M. Prior and R. Marrus, Phys. Rev. Lett. 49, 1329 (1982).
5. R. Mann, C. L. Cocke, A. S. Schlachter, M. Prior and R. Marrus, Phys. Rev. Lett. 49, 1329 (1982).
6. J. B. Marion and F. C.Young, Nuclear Reaction Analysis Graphs and Tables, (North-Holland, Amsterdam, 1968), pp. 140-142.
7. C. E. Moore, Atomic Energy Levels, Natl. Bur. Stand. (U.S.) Circular No. 467 (U.S. GPO, Washington, D.C. 1971).
8. S. Baskin and J. O. Stoner, Jr., Atomic Energy Levels and Grotrain Diagrams (North-Holland, Amsterdam, 1975).
9. R. Mann, C. L. Cocke, A. S. Schlachter, M. Prior and R. Marrus, Phys. Rev. Lett. 49, 1329 (1982).
10. E. Justiniano, Ph.D. Dissertation (Kansas State University, 1982).
11. R. E. Olson and A. Salop, Phys. Rev. A 14, 579 (1976).
12. C. Zener, Proc. Roy. Soc. A 137, 696 (1932).
13. H. Ryufuku, K. Sasaki, and T. Watanabe, Phys. Rev. A 21, 745 (1980).
14. R. Mann, F. Folkmann, and H. F. Beyer, J. Phys. B: Atom. Molec. Phys. 14, 1161 (1981).
15. R. Mann, H. F. Beyer, and F. Folkmann, Phys. Rev. Lett. 46, 646 (1981).
16. H. F. Beyer, K. H. Schartner, and F. Folkmann, J. Phys. B: Atom. Molec. Phys. 13, 2459 (1980).

17. R. E. Olson and A. Salop, Phys. Rev. A 14, 579 (1976).

18. C. Zener, Proc. Roy. Soc. A 137, 696 (1932).

19. R. E. Olson and A. Salop, Phys. Rev. A 14, 579 (1976).

20. E. Justiniano, Ph.D. Dissertation (Kansas State University, 1982).

21. E. Justiniano, Ph.D. Dissertation (Kansas State University, 1982).

22. R. Mann, C. L. Cocke, A. S. Schlachter, M. Prior and R. Marrus, Phys. Rev. Lett. 49, 1329 (1982).

APPENDIX A

CALCULATION OF ANALYZER CONSTANT K

Figure 1A depicts two concentric hemispheres of radii R_1 and R_2. If we neglect boundary effects from either end of the hemisphere, the total potential of each hemisphere is given by

$$V_1 = \frac{Q}{4\pi\varepsilon_0 R_1} \tag{A1}$$

$$V_2 = \frac{Q}{4\pi\varepsilon_0 R_2} \tag{A2}$$

where Q is the magnitude of the total charge on the inner hemisphere. The potential difference, ΔV, is then given by

$$\Delta V = V_1 - V_2 \tag{A3}$$

$$= (Q/4\pi\varepsilon_0)\left(\frac{1}{R_1} - \frac{1}{R_2}\right) \tag{A4}$$

Solving for Q yields

$$Q = (4\pi\varepsilon_0)\Delta V/\left(\frac{1}{R_1} - \frac{1}{R_2}\right) \tag{A5}$$

$$= R_1 R_2 (4\pi\varepsilon_0)\Delta V/R_2 - R_1. \tag{A6}$$

We now consider an ion (of charge q) traversing a path through the analyzer at radius R. Using Newton's second law (F=ma), where F is the electrostatic force $\left(\frac{Qq}{4\pi\varepsilon_0 R^2}\right)$ and a is the centripetal acceleration $\left(\frac{v^2}{R}\right)$ yields

$$Qq/4\pi\varepsilon_0 R^2 = mv^2/R \tag{A7}$$

Figure A1: Schematic representation of hemispherical double-focusing spectrometer.

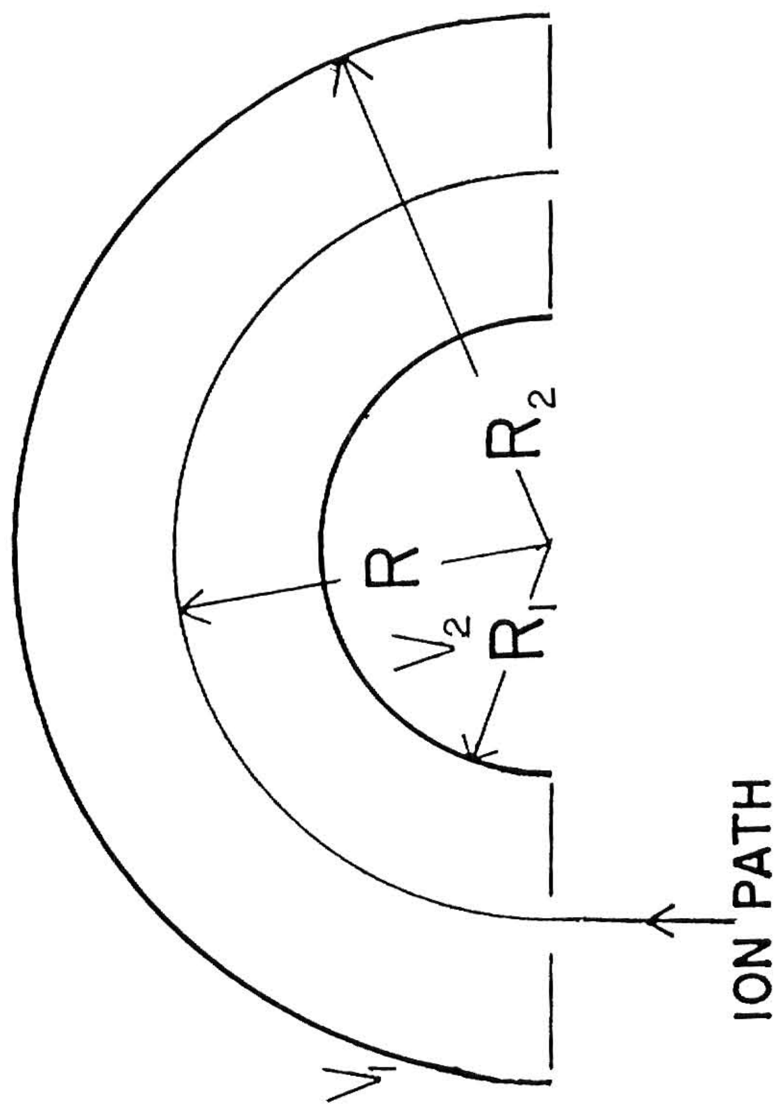
R
R_2
R_1
V_2
V_1
ION PATH

which reduces to

$$E/q = Q/2(4\pi\varepsilon_0)R \tag{A8}$$

by using $E = \frac{1}{2}mv^2$. Substituting the value of Q from Eq. (A6) yields

$$E/q = \Delta V \; R_1R_2/2R(R_2 - R_1). \tag{A9}$$

with

$$\frac{1}{K} = R_1R_2/2R(R_2 - R_1) \tag{A10}$$

we now have Eq. (1a) and (1b) of Chapter II.

$$\Delta V = K\,\frac{E}{q} \tag{A11}$$

Measured values of R_1, R_2 and R are 28, 69 and 48mm respectively. This yields a K of 2.04. The experimentally determined K was 1.21±.02.

APPENDIX B

```
]LIST #0   KINEMA 1

10  HOME
20  PRINT "DO YOU WISH TO USE THE
      MASS OF NEON AND THE MASS O
     F HELIUM ?": INPUT A$: IF A$
      = "Y" THEN  GOTO 60
*30 : INPUT "M2
          =";M2
50  GOTO 70
60 M1 = 20.179:Z2 = 1:M2 = 4.0026

70  INPUT "Q IN =";QI: INPUT "VAC
     C=";VA
71  INPUT "Q=";Q
72  HOME
73  INPUT "PROJECTILE SCATTERING
     ANGLE IN DEGREES ";PHI
74 PHI = PHI / 57.296
75 E1 = QI * VA
120 ET = E1 + Q
130 A = M1 * M1 * (E1 / ET) / ((M
     1 + M2) * (M2 + M1))
140 B = M1 * M2 * (E1 / ET) / ((M
     1 + M2) * (M2 + M1))
150 C = M2 * M2 * (1 + M1 * Q / (
     M2 * ET)) / ((M1 + M2) * (M2
      + M1))
160 D = M2 * M1 * (1 + M1 * Q / (
     M2 * ET)) / ((M1 + M2) * (M2
      + M1))
170 E4 = ET * A * ( COS (PHI) +  SQR
     (C / A - ( SIN (PHI)) ^ 2)) ^
     2
180 DE = E4 - E1
190 W =  SQR (M1 * E4 / (M2 * ET *
     D)) *  SIN (PHI)
200 THETA =  ATN (W /  SQR ( - W *
     W + 1))
202  PRINT "DELTA E = "DE
203  PRINT
204 THETA = THETA * 57.296
206  PRINT "THETA CENTER OF MASS
     = "THETA
208  PRINT
210  PRINT "ANOTHER SCATTERING AN
     GLE?": INPUT W$: IF W$ = "Y"
      THEN  GOTO 72
215  PRINT
220  PRINT "OTHER Q VALUE": INPUT
     X$: IF X$ = "Y" THEN  GOTO 7
     1
225  PRINT "ANOTHER VACC ?": INPUT
     R$: IF R$ = "Y" THEN  GOTO 7
     0
230  END
```

```
]LIST   KINEMA

10  HOME
15  DEF  FN A(X) =  ATN (X /  SQR
     ( - X * X + 1))
20  PRINT "DO YOU WISH TO USE THE
      MASS OF NEON AND THE MASS O
     F HELIUM ?": INPUT A$: IF A$
      = "Y" THEN  GOTO 60
30 : INPUT "M2
          =";M2
50  GOTO 70
60 M1 = 20.179:Z2 = 1:M2 = 4.0026

70  INPUT "Q IN =";QI
71  INPUT "VACC = ";VA
72  INPUT "Q VALUE = ";Q
73  HOME
74 F = 0
75 E1 = QI * VA
77 Z1 = QI - 1
80 E0 = 1.602E - 19
85 K = 8.99E9
90 RX = Z1 * Z2 * K * E0 / Q
100 B0 = Z1 * Z2 * K * E0 * (M1 +
     M2) / (E1 * M2)
107 Y = (2 * (RX / B0)) - 1
110 THETA =  ATN (1 /  SQR (Y * Y
     - 1)) + ( SGN (Y) - 1) * 1.
     5708
115 THETA =  ABS (THETA)
120 ET = E1 + Q
130 A = M1 * M1 * (E1 / ET) / ((M
     1 + M2) * (M2 + M1))
140 B = M1 * M2 * (E1 / ET) / ((M
     1 + M2) * (M2 + M1))
150 C = M2 * M2 * (1 + M1 * Q / (
     M2 * ET)) / ((M1 + M2) * (M2
      + M1))
160 D = M2 * M1 * (1 + M1 * Q / (
     M2 * ET)) / ((M1 + M2) * (M2
      + M1))
170 E3 = ET * (B + D - 2 *  SQR (
     A * C) *  COS (THETA))
180 E4 = ET * (A + C + 2 *  SQR (
     A * C) *  COS (THETA))
185 W =  SQR (ET * D / E3) *  SIN
     (THETA)
190 CHI =  ATN (W /  SQR ( - W *
     W + 1))
195 P =  SQR (M2 * E3 / (M1 * E4)
     ) *  SIN (CHI)
200 PHI =  ATN (P /  SQR ( - P *
     P + 1))
210  PRINT "THE ENERGY OF THE HEA
     VY PARTICLE IN EV = "E4
215  PRINT
220 CHI = CHI * 57.296
230 PHI = PHI * 57.296
240  PRINT "AT AN ANGLE IN DEGREE
     S OF "PHI
245  PRINT
250  PRINT "ENERGY OF THE LIGHT P
     ARTICLE IN EV = "E3
```

```
255  PRINT
260  PRINT "AT AN ANGLE IN DEGREE
     S OF "CHI
261  PRINT
262 DE = E4 - E1
263  PRINT "DELTA E = "DE
264  PRINT
266  IF F = 1 THEN  GOTO 350
267  IF F = 0 THEN  GOTO 320
268  PRINT
270  PRINT "WOULD YOU LIKE VALUES
      FOR RX/N": INPUT N$: IF N$ =
     "N" THEN  GOTO 370
275  PRINT
280  PRINT "VALUE OF N": INPUT N
285  PRINT
290 RX = RX / N
295  HOME
300  GOTO 107
320 F = 1
330 R = RX
340  GOTO 270
350 RX = R
360  GOTO 270
370  PRINT
380  PRINT "WOULD YOU LIKE TO FIN
     D VALUES FOR DIFFERENT Q VAL
     UES ": INPUT X$: IF X$ = "Y"
      THEN  GOTO 72
390  PRINT
400  PRINT "VALUES FOR DIFFERENT
     VACC ": INPUT R$: IF R$ = "Y
     " THEN  GOTO 71
410  PRINT
420  PRINT "VALUES FOR DIFFERENT
     Q IN ": INPUT S$: IF S$ = "Y
     " THEN  GOTO 70
430  PRINT
440  END
```

APPENDIX C

]LIST SCIPLOT

```
10  HIMEM: 38399: LOMEM: 24576:CD
     $ =  CHR$ (4): IF  PEEK (147
     20) +  PEEK (16367) <  > 96 THEN
      PRINT CD$;"BLOAD PKWDATA,A1
     4720"
12  DIM IN$(50),D(2400):MAX = 240
     0
15  POKE 232,128: POKE 233,57:STA
     R$ = "********** "
20  SCALE= 1: ROT= 0
25 D2$ = ",D2":D1$ = ",D1"
94  DEF  FN H8(X) = ( LOG (X) - L
     0) * DX / (L1 - L0) + XL
95  DEF  FN H9(Y) = (( LOG (Y) -
     L2) * DY / (L3 - L2)) + YB
96  HGR2 : TEXT : HOME
97  DEF  FN XN(X) = (X - X0) * XX
      + XL
98  DEF  FN YN(Y) = (Y - Y0) * YY
      + YB
99  POKE 51,0: ONERR  GOTO 3100
100 S = 0:S$ = "READ FORMAT FILE
     NAME":RG$ = "":IN$(S) = "NON
     E": GOSUB 2000: IF A$ = "" GOTO
     115
110  PRINT CD$;"OPEN ";IN$(S);D1$
     : PRINT CD$;"READ ";IN$(S): INPUT
     NS: FOR I = 1 TO NS: INPUT I
     N$(I): NEXT : PRINT CD$;"CLO
     SE ";IN$(S)
115  GOTO 700
120  PRINT STAR$;"DEFINE AXES"
130 S = 1:S$ = "COLOR OF AXES":RG
     $ = "0:7": GOSUB 2000: HCOLOR=
     V0
135  PRINT "DEFINE X AXIS"
140 S = 2:S$ = "POSITION OF LEFT
     END":RG$ = "0:279:10:181": GOSUB
     2000:XL = V0:YL = V1
150 S = 3:S$ = "POSITION OF RIGHT
      END": GOSUB 2000:XR = V0:YR
      = YL
160  HPLOT XL,YL TO XR,YR:DX = XR
      - XL
170 S = 4:S$ = "MINIMUM X VALUE":
     RG$ = "": GOSUB 2000:X0 = V0

180 S = 5:S$ = "MAXIMUM X VALUE":
     GOSUB 2000:X1 = V0
190 S = 6:S$ = "LOG SCALE":RG$ =
     "Y:N": GOSUB 2000:XG = 0: IF
     IN$(S) <  > "Y" GOTO 230
210 XG = 1
220 L0 = XG *  LOG (X0):L1 = XG *
      LOG (X1)
225  GOTO 310
230 S = 8:S$ = "VALUE OF FIRST LA
     BEL":RG$ =  STR$ (X0) + ":" +
      STR$ (X1): GOSUB 2000:MX =
     V0
240 S = 9:S$ = "INTERVAL BETWEEN
     LABELS":RG$ = "0:" +  STR$ (
     X1 - X0): GOSUB 2000:IX = V0

250 NL = (X1 - MX) / IX:XX = DX /
     (X1 - X0):LX =  LEN ( STR$ (
      INT (MX))) -  LEN (IN$(8))
```

```
255  IF NL > 25 THEN  PRINT "TOO
     MANY LABELS": GOTO 230
257  GOSUB 2200:ML =  LEN ( STR$
     ( INT (MX + NL * IX))) - LX +
     1:X4 = XR -  FN XN(MX)
260 YP = 9:Y2 = 0: IF NL > X4 / (
     ML * 8) THEN YP = 13:Y2 =  -
     4
262  IF YL < 90 THEN YP =  - 2:Y2
      = 0: IF NL > X4 / (ML * 8) THEN
     YP =  - 6:Y2 = 4
264 YP = YL + YP: ROT= 0:RT = 0
270  IF NL > X4 / (ML * 4) THEN Y
     P = YL + 3:Y2 = 0: ROT= 16:R
     T = 16
300  FOR X2 = MX TO X1 STEP IX:Y3
      = YP + Y2:Y2 =  - Y2:X3 =  FN
     XN(X2)
305  DRAW 2 AT X3,YL: GOSUB 2310:
      NEXT X2: TEXT : GOTO 370
310 JC = L0 /  LOG (10):JL% =  INT
     (JC - .001) + 1:LX = 0
315 JC = L1 /  LOG (10):JM% =  INT
     (JC): GOSUB 2200
317 Y3 = YL + 9: IF YL < 90 THEN
     Y3 = YL - 2
320  FOR JC = JL% TO JM%:X2 = 10 ^
     JC:X3 =  FN H8(X2)
325  DRAW 2 AT X3,YL: GOSUB 2310:
      NEXT JC
330 JL% = JL% - 1: FOR JC = JL% TO
     JM%:YR = 10 ^ JC
335  FOR JL = 2 TO 9:X2 = JL * YR

340  IF X2 < X0 THEN 355
345  IF X2 > X1 THEN 355
350 X3 =  FN H8(X2): DRAW 1 AT X3
     ,YL
355  NEXT JL
360  NEXT JC
365  TEXT : GOTO 400
370 S = 11:S$ = "TICK MARK INTERV
     AL":RG$ = "0:" +  STR$ (X1 -
     X0): GOSUB 2000:JX = V0: GOSUB
     2200
380  FOR X2 = MX - (JX *  INT ((M
     X - X0) / JX + .1)) TO X1 STEP
     JX: DRAW 1 AT  FN XN(X2),YL:
      NEXT : TEXT
400  PRINT "DEFINE Y AXIS"
410 S = 12:S$ = "POSITION OF BOTT
     OM END":RG$ = "18:261:0:191"
      GOSUB 2000:XB = V0:YB = V1

420 S = 13:S$ = "POSITION OF TOP
     END": GOSUB 2000:XT = XB:YT =
     V1
430  HPLOT XB,YB TO XT,YT:DY = YT
      - YB
435 AUT% = AUT:AUT = 0
440 S = 14:S$ = "MINIMUM Y VALUE"
     :RG$ = "": GOSUB 2000:Y0 = V
     0
450 S = 15:S$ = "MAXIMUM Y VALUE"
     : GOSUB 2000:Y1 = V0
455 YG = 0:
460 S = 16:S$ = "LOG SCALE":RG$ =
     "Y:N": GOSUB 2000:YG = 0: IF
     IN$(S) <  > "Y" GOTO 500
480 YG = 1
490 L2 = YG *  LOG (Y0):L3 = YG *
      LOG (Y1)
```

```
495  GOTO 540
500 S = 18:S$ = "VALUE OF FIRST L
    ABEL":RG$ =  STR$ (Y0) + ":"
     +  STR$ (Y1): GOSUB 2000:MY
     = V0: ROT= 0
510 S = 19:S$ = "INTERVAL BETWEEN
     LABELS":RG$ = "0:" +  STR$
    (Y1 - Y0): GOSUB 2000:IY = V
    0
520 NL = (Y1 - MY) / IY:YY = DY /
    (Y1 - Y0):LY =  LEN ( STR$ (
     INT (MY))) -  LEN (IN$(18))
      IF NL > 15 THEN  PRINT "TO
    O MANY LABELS":AUT = 0: GOTO
    500
530  GOSUB 2200: FOR Y2 = MY TO Y
    1 STEP IY:Y3 =  FN YN(Y2)
534  DRAW 2 AT XB,Y3
536  GOSUB 2540: NEXT Y2
538  TEXT : GOTO 600
540 JC = L2 /  LOG (10):JL% =  INT
    (JC - .001) + 1
545 JC = L3 /  LOG (10):JM% =  INT
    (JC):LY = 0
550  GOSUB 2200
555  FOR JC = JL% TO JM%:Y2 = 10 ^
    JC:Y3 =  FN H9(Y2)
560  DRAW 2 AT XB,Y3: GOSUB 2540:
     NEXT JC
565 JL% = JL% - 1: FOR JC = JL% TO
    JM%
570 YR = 10 ^ JC: FOR JL = 2 TO 9

575 Y2 = JL * YR: IF Y2 < Y0 THEN
    590
580  IF Y2 > Y1 THEN 590
585 Y3 =  FN H9(Y2): DRAW 1 AT XB
    ,Y3
590  NEXT JL
595  NEXT JC
596 Y0 =  LOG (Y0):Y1 =  LOG (Y1)
     YY = DY / (Y1 - Y0)
597  TEXT :AUT = AUT%: GOTO 680
600 S = 20:S$ = "TICK MARK INTERV
    AL":RG$ = "0:" +  STR$ (Y1 -
    Y0): GOSUB 2000:JY = V0: GOSUB
    2200
610  FOR Y2 = MY - (JY *  INT ((M
    Y - Y0) / JY)) TO Y1 STEP JY
    : DRAW 1 AT XB, FN YN(Y2): NEXT
    : TEXT
615 AUT = AUT%
620 S = 21:S$ = "DRAW GRID DOTS":
    RG$ = "Y:N": GOSUB 2000: IF
    IN$(S) <  > "Y" GOTO 680
640  GOSUB 2200: FOR X2 = MX - (J
    X *  INT ((MX - X0) / JX)) TO
    X1 STEP JX:X3 =  FN XN(X2)
660  FOR Y2 = MY - (JY *  INT ((M
    Y - Y0) / JY)) TO Y1 STEP JY
    :Y3 =  FN YN(Y2)
670  HPLOT X3,Y3: NEXT : NEXT : TEXT

680 S = 22:S$ = "FRAME AXES":RG$ =
    "Y:N": GOSUB 2000: IF IN$(S)
     <  > "Y" GOTO 700
690  HPLOT XL,YB TO XL,YT TO XR,Y
    T TO XR,YB TO XL,YB
695  GOTO 1000
700  PRINT STAR$;"INPUT DATA"
702  IF D(0) > 0 AND AUT = 0 THEN
    S = 28:S$ = "USE SAME DATA":
     GOSUB 2000: IF IN$(S) = "Y"
     THEN  GOTO 704
```

```
703  GOTO 710
704  PRINT "JUST RECALCULATE ENER
     GY GAIN VALUES (Y/N)?": INPUT
     T$: IF T$ = "Y" THEN XT = 1:
      GOTO 7010
705  GOTO 880
710 XY = 2:BT = 2:EB = 0
711 XT = 0
715 AUT% = AUT:AUT = 0
717  IF BT = 1 THEN  PRINT "BACKG
     ROUND RUN "
720 S = 25:S$ = "READ DATA FILE N
     AME":RG$ = "": GOSUB 2000: IF
     IN$(S) = "" OR IN$(S) = "NON
     E" GOTO 820
725 AUT = AUT%
730 D1 = 1
740 DD = 2
745  ONERR  GOTO 810
750  PRINT CD$;"OPEN ";IN$(25);D2
     $: PRINT CD$;"READ ";IN$(25)
     : INPUT D(0): PRINT D(0);" V
     ALUES IN ";IN$(25)
760 D = 0:ND = 1: FOR I = D1 TO D
     (0)
770 ND = 2 * I: IF BT = 1 THEN  GOTO
     775
772  INPUT D(ND): GOTO 795
775  INPUT YD:D(ND) = D(ND) - YD *
     FA: IF D(ND) < 0 THEN D(ND) =
     0: GOTO 795
795  NEXT
800  PRINT CD$;"CLOSE ";IN$(25): POKE
     216,0
810  GOSUB 7000: GOTO 880
820 S = 10:S$ = "DATA CALCULATION
      SUBROUTINE":RG$ = "0:9000":
      GOSUB 2000
825 SB =  INT ((V0 + 1) / 1000): ON
     SB GOSUB 2999,2999,3000,4000
     ,5000,6000,7000,8000,9000: IF
     SB > 2 GOTO 880
830  PRINT "TYPE Y=9999 TO END IN
     PUT":ND = 0:RG$ = "":S = 0:D
      = 1
840 ND = ND + 1: PRINT "POINT "ND

845  IF XY = 2 THEN S$ = "X VALUE
     ":IN$(S) =  STR$ (D(D)): GOSUB
     2000:D(D) = V0:D = D + 1
850 S$ = "Y VALUE":IN$(S) =  STR$
     (D(D)): GOSUB 2000:D(D) = V0
     :D = D + 1: IF V0 = 9999 GOTO
     870
860  IF EB = 1 THEN S$ = "+/- ERR
     OR":IN$(S) =  STR$ (D(D)): GOSUB
     2000:D(D) = V0:D = D + 1
865  IF D < MAX - XY GOTO 840
870 D(0) = D - XY - 1
880  PRINT STAR$;"SCALE DATA": IF
     XY = 1 GOTO 885
881  PRINT "CR TO SKIP": INPUT T$
     : IF T$ = "" THEN  GOTO 130
882 X2 = D(1):X3 = X2: FOR I = 1 TO
     2 * D(0) STEP XY + EB: IF D(
     I) < X2 THEN X2 = D(I)
883  IF D(I) > X3 THEN X3 = D(I)
884  NEXT : PRINT "MINIMUM AND MA
     XIMUM X VALUES ARE ";X2;":";
     X3
885 Y2 = D(XY):Y3 = Y2: FOR I = X
     Y + 4 TO 2 * D(0) STEP XY +
     EB: IF D(I) < Y2 THEN Y2 = D
     (I)
```

```
886  IF D(I) > Y3 THEN Y3 = D(I)
888  NEXT : PRINT "MINIMUM AND MA
     XIMUM Y VALUES ARE ";Y2;":";
     Y3
995  GOTO 130
1000  PRINT STAR$;"PLOT DATA"
1001 CT = 1
1002 S = 36:S$ = "SYMBOL #":RG$ =
     "1:20": GOSUB 2000:SY = V0
1004 S = 37:S$ = "SOLID SYMBOLS":
     RG$ = "Y:N": GOSUB 2000:S0 =
     SY: IF IN$(S) = "Y" THEN S0 =
      INT ((SY - 1) / 4) * 4 + 1
1006 S = 38:S$ = "SYMBOL COLOR":R
     G$ = "0:7": GOSUB 2000: HCOLOR=
     V0
1010 S = 39:S$ = "CONNECTING LINE
     S":RG$ = "Y:N": GOSUB 2000:C
     P = 0: IF IN$(S) = "Y" THEN
     CP = 1
1020  GOSUB 2200:XT = XF - XI: FOR
     I = 1 TO 2 * D(0) STEP XY +
     EB:X2 = D(I): IF XY = 1 THEN
     X2 = XT + XI:XT = X2
1022  IF XG < > 1 THEN 1030
1024 X3 =  FN H8(X2): IF X3 < XL THEN
     1130
1026  GOTO 1035
1030 X3 =  FN XN(X2): IF X3 < XL GOTO
     1130
1035  IF X3 > XR GOTO 1190
1040 Y3 =  FN YN(D(I + XY - 1)): IF
     Y3 > YB OR Y3 < YT GOTO 1130

1050  FOR S = S0 TO SY: DRAW S AT
     X3,Y3: NEXT : IF CP = 0 GOTO
     1090
1060  IF CT = 1 THEN  GOTO 1080
1070  HPLOT X4,Y4 TO X3,Y3
1080 X4 = X3:Y4 = Y3
1081 CT = CT + 1
1090  IF EB = 0 GOTO 1140
1100 Y2 =  FN YN(D(I + XY - 1) -
     D(I + XY)): IF Y2 > YB OR Y2
      < YT GOTO 1130
1110 Y3 =  FN YN(D(I + XY - 1) +
     D(I + XY)): IF Y3 > YB OR Y3
      < YT GOTO 1130
1120  HPLOT X3,Y2 TO X3,Y3: DRAW
     1 AT X3,Y2: DRAW 1 AT X3,Y3:
      GOTO 1140
1130  PRINT "WHEE,IM PLOTTING"
1140  NEXT I: TEXT
1190  TEXT :AUT = 0
1200  PRINT STAR$;"LABEL GRAPH":S
      = 40
1202 S$ = "LABEL " +  STR$ (S - 3
     9):RG$ = "": GOSUB 2000
1210  GOSUB 2200:A$ = IN$(S): FOR
     I = 1 TO A:C =  ASC ( MID$ (
     A$,I,1))
1220  IF C = 64 THEN  GOSUB 2100:
     X3 = V0: GOSUB 2100: DRAW 17
      AT X3,V0: XDRAW 17: GOTO 12
     20
1230  IF C = 38 THEN  GOSUB 2100:
     ROT= V0 * 16: GOTO 1220
1240  IF C = 35 THEN  GOSUB 2100:
     HCOLOR= V0: GOTO 1220
1250  IF C = 36 THEN  GOSUB 2100:
     I = I - 1:C = V0: IF I = A -
     1 THEN I = A
1260  DRAW C: NEXT : TEXT :S = S +
     1: IF S < 45 GOTO 1202
```

```
1265  PRINT "ARE LABELS OK(Y/N)?"
       INPUT T$: IF T$ = "N" THEN
      GOTO 1200
1965  PRINT STAR$;"SAVE FILES":AU
      T = 0
1970 S = 45:S$ = "WRITE DATA FILE
      NAME":RG$ = "":IN$(S) = "NO
     NE": GOSUB 2000: IF A$ = "" GOTO
     1985
1975  PRINT CD$;"OPEN ";IN$(S);: PRINT
     D1$: PRINT CD$;"WRITE ";IN$(
     S): FOR I = 0 TO D(0): PRINT
     D(I): NEXT : PRINT CD$;"CLOS
     E ";IN$(S)
1985 S = 46:S$ = "WRITE FORMAT FI
     LE NAME":RG$ = "":IN$(S) = "
     NONE": GOSUB 2000: IF A$ = "
     " GOTO 1992
1990  PRINT CD$;"OPEN ";IN$(S);: PRINT
     D1$: PRINT CD$;"WRITE ";IN$(
     S): PRINT S
1991  FOR I = 1 TO S: PRINT  CHR$
     (34);IN$(I); CHR$ (34): NEXT
     : PRINT CD$;"CLOSE ";IN$(S)
1992 S = 47:S$ = "WRITE PICTURE F
     ILE NAME":IN$(S) = "NONE": GOSUB
     2000: IF IN$(S) = "NONE" GOTO
     1994
1993  PRINT CD$;"BSAVE ";IN$(S);"
     ,A$4000,L$1FFF,D1"
1994 S = 48:S$ = "READ PICTURE FI
     LE NAME":IN$(S) = "NONE": GOSUB
     2000: IF IN$(S) = "NONE" GOTO
     1996
1995  GOSUB 2200: PRINT CD$;"BLOA
     D ";IN$(S);",A$4000,D1": TEXT
     : GOTO 1994
1996  IF CV = 6 THEN  RETURN
1997 S = 49:S$ = "ERASE GRAPH":RG
     $ = "Y:N": GOSUB 2000: IF IN
     $(S) = "Y" GOTO 96
1998 S = 50:S$ = "MODIFY AXES": GOSUB
     2000: IF IN$(S) = "Y" GOTO 1
     00
1999  GOTO 700
2000  PRINT S$;"(";RG$;")? (";IN$
     (S);")";: GOSUB 2800:OK = 0:
      IF A > 0 THEN IN$(S) = A$: GOTO
     2020
2005 A =  LEN (IN$(S)): IF A = 0 GOTO
     2090
2010  FOR I = 1 TO A: IF  MID$ (I
     N$(S),I,1) = "," THEN B = I +
     1
2015  NEXT
2020 L =  LEN (RG$): IF L = 0 GOTO
     2095
2030 R$ = "":R = 0: FOR J = 1 TO
     L
2035  IF  MID$ (RG$,J,1) <  > ":"
      THEN R$ = R$ +  MID$ (RG$,J
     ,1): IF J < L GOTO 2080
2040  IF  VAL (R$) = 0 AND  ASC (
     R$) <  > 48 GOTO 2060
2042  IF R = 0 THEN V0 =  VAL (IN
     $(S)): IF V0 <  VAL (R$) GOTO
     2070
2044  IF R = 1 THEN  IF V0 >  VAL
     (R$) GOTO 2070
2046  IF R = 2 THEN V1 =  VAL ( MID$
     (IN$(S),B)): IF V1 <  VAL (R
     $) GOTO 2070
2048  IF R = 3 THEN  IF V1 >  VAL
     (R$) GOTO 2070
```

```
2050 R = R + 1:OK = 1:R$ = "": GOTO
     2080
2060  IF IN$(S) <  > R$ THEN R$ =
     "": GOTO 2080
2065 OK = 1: GOTO 2075
2070 OK = 0
2075 J = L
2080  NEXT
2090  IF OK = 0 THEN  PRINT  CHR$
     (7);"INVALID ENTRY; CHECK (R
     ANGE)":AUT = 0: GOTO 2000
2095 V0 =  VAL (IN$(S)): RETURN
2100 I = I + 1:V0 = I
2110 I = I + 1: IF I > (A) THEN J
      = I:I = I - 1: GOTO 2120
2115 C =  ASC ( MID$ (A$,I,1)): IF
     C > 47 AND C < 58 GOTO 2110
2116 J = I
2120 V0 =  VAL ( MID$ (A$,V0,J -
     V0)): RETURN
2200  POKE  - 16304,0: POKE  - 16
     299,0: RETURN
2310 X2$ =  STR$ (X2): IF LX = 0 GOTO
     2330
2320 X2$ =  STR$ (X2 +  SGN (X2) *
     10 ^ LX):L =  LEN ( STR$ ( INT
     (X2))) - LX: IF  ABS (X2) <
     1 THEN L = L - 1
2325 X2$ =  LEFT$ (X2$,L)
2330 L =  LEN (X2$): IF RT = 0 THEN
     X3 = X3 - 4 * L: GOTO 2340
2335 X3 = X3 - 3
2340  DRAW  ASC (X2$) AT X3,Y3: IF
     L = 1 GOTO 2360
2350  FOR I = 2 TO L: DRAW  ASC (
      MID$ (X2$,I,1)): NEXT
2360  RETURN
2540 Y2$ =  STR$ (Y2): IF LY = 0 GOTO
     2570
2550 Y2$ =  STR$ (Y2 +  SGN (Y2) *
     10 ^ LY):L =  LEN ( STR$ ( INT
     (Y2))) - LY: IF  ABS (Y2) <
     1 THEN L = L - 1
2560 Y2$ =  LEFT$ (Y2$,L)
2570 L =  LEN (Y2$):Y3 = Y3 + 3:X
     3 = XB + 2: IF XB < 160 THEN
     X3 = XB - 2 - 8 * L
2572  IF Y3 > YB THEN Y3 = YB
2575  DRAW  ASC (Y2$) AT X3,Y3: IF
     L = 1 GOTO 2590
2580  FOR I = 2 TO L: DRAW  ASC (
      MID$ (Y2$,I,1)): NEXT
2590  RETURN
2800 A = 0:B = 0:A$ = "": IF AUT =
     1 AND  PEEK ( - 16384) < 128
      THEN  PRINT : RETURN
2805 AUT = 0
2810  GET C$:C =  ASC (C$): IF C >
     31 GOTO 2880
2815  IF C <  > 8 GOTO 2820
2816  PRINT C$;: IF A < 2 GOTO 28
     00
2818 A = A - 1:A$ =  LEFT$ (A$,A)
      GOTO 2810
2820  IF C = 13 THEN  PRINT : RETURN

2825  IF C = 1 THEN AUT = 1: GOTO
     2800
2826  IF C = 2 THEN AUT = 0: GOTO
     96
2828  IF C = 4 THEN  PRINT : PRINT
     CD$;A$: POP : GOTO 2000
```

```
2829  IF C = 6 THEN SV = S:CV = C
     :ZV$ = S$:TV$ = RG$: PRINT :
      GOSUB 1965: POP :S = SV:S$ =
     ZV$:RG$ = TV$:CV = 0: GOTO 2
     000
2830  IF C = 7 THEN  GOSUB 2200: GOTO
     2810
2840  IF C = 20 THEN  TEXT : GOTO
     2810
2850  IF C = 24 THEN  PRINT  CHR$
     (92): GOTO 2800
2852  IF C = 16 THEN  GET C$: PRINT
     : PRINT CD$ + "PR# " + C$: GOTO
     2810
2855  IF C = 26 THEN  POP : POP :
      GOTO 1965
2858  IF C = 17 THEN  PRINT  CHR$
     (9)"G2D": GOTO 2810
2859  IF C = 18 THEN  TEXT : PRINT
     : PRINT CD$;"RUN MENU";D1$: END

2860  IF C = 3 THEN  GOSUB 2900:C
      =  LEN (A$):A$ = A$ +  STR$
     (XC) + ",":B =  LEN (A$) + 1
     :A$ = A$ +  STR$ (YC):A =  LEN
     (A$): PRINT  MID$ (A$,C + 1)
     ;
2870  GOTO 2810
2880  IF C = 44 THEN B = A + 2
2890  PRINT C$;:A = A + 1:A$ = A$
      + C$: GOTO 2810
2900  GOSUB 2200
2905 XC =  INT ( PDL (0) * 1.098)
     : FOR I = 1 TO 10: NEXT :YC =
      INT ( PDL (1) * .75)
2910  XDRAW 2 AT XC,YC: FOR I = 1
      TO 50: NEXT : XDRAW 2 AT XC
     ,YC
2920  IF  PEEK ( - 16384) < 128 GOTO
     2905
2930  GET C$: TEXT : RETURN
2999  RETURN
3000 D(0) = 200: FOR I = 1 TO D(0
     ):D(I) =  SIN (I / 10): NEXT
     : RETURN
3100  PRINT : PRINT CD$"CLOSE ": TEXT
     : PRINT CD$"PR#0": PRINT  CHR$
     (7)"ERROR " PEEK (222)" IN L
     INE " PEEK (218) + 256 *  PEEK
     (219): GOTO 1965
7000  REM  ROUTINE TO CALCULATE X
      VALUES(Q)
7003  IF BT = 1 THEN  GOTO 7065
7005  PRINT "DO YOU WANT TO SUBTR
     ACT BACKGROUND(Y/N)? ": INPUT
     T$: IF T$ = "Y" THEN BT = 1:
      INPUT "FACTOR? ";FA: GOTO 7
     020
7012  IF XT = 1 GOTO 7073
7015  IF BT = 1 GOTO 7065
7020 DM = 1: FOR I = 4 TO D(0):J =
     2 * I: IF D(J) > DM THEN DM =
     D(J):IM = I
7031  NEXT
7040 Z = 0:SU = 0
7045  FOR I = IM - 10 TO IM + 10:
     J = 2 * I:SU = SU + I * D(J)
     :Z = Z + D(J): NEXT
7050 IB = SU / Z
7060  PRINT "IMAX=";IM;"  IAV=";I
     B: IF BT = 1 THEN  GOTO 715
```

```
7065 YM = 0: FOR I = IM + 10 TO D
     (0): IF YM < D(2 * I) THEN Y
     M = D(2 * I)
7067  NEXT : PRINT "MAX COUNTS AB
     OVE MAIN PEAK = ";YM
7068  INPUT "QIN";Q: INPUT "QOUT"
     ;QP: INPUT "VR0";VM: INPUT "
                 VR0 CH#";VX: INPUT
     "VR";VR: INPUT "VR CH#";VY: INPUT
     "DELV";DLV: INPUT "VCELL";VL
     : INPUT "ANALYZER CONSTANT="
     ;K
7069 AL = (VR - VM) / (VY - VX)
7070 VA = (IB - 1) * AL + (VM - A
     L * VX) + DLV / K + VL
7071  PRINT "V/CH="AL
7072  PRINT "VACC="VA
7073 Q0 = VA * (QP - Q)
7075  PRINT "DO YOU WANT TO CHANG
     E IAV?": INPUT T$: IF T$ = "
     Y" THEN  INPUT "IB?";IB
7080  FOR I = 1 TO D(0):J = 2 * I
      - 1:QV = (I - IB) * AL * QP
      + Q0
7090 D(J) = QV: NEXT
7205 T$ = "#3@185,8&0" + IN$(25)
7206 IN$(44) = T$
7210  INPUT "PROJECTILE? ";P$: INPUT
     "TARGET? ";T$
7220 IN$(43) = "#3@170,25&0" + P$
      + " ON " + T$
7300  RETURN
```

APPENDIX D

EVALUATION OF SPECTRAL RESOLUTION

Recall Eq. (3) in Chapter II

$$E_G = q'(V_R - V_R^o) + (V_o + V_c)(q' - q) \tag{D1}$$

with

$$V_o + V_c = V_{acc}. \tag{D2}$$

V_{acc} can also be written as

$$V_{acc} = V_R^o + V_c + \Delta V/K \tag{D3}$$

where $\Delta V/K$ is the energy per charge of the analyzed ion. Substituting (D3) into (D1) yields

$$E_G = q'(V_R + V_c + \Delta V/K) - q\, V_{acc}. \tag{D4}$$

If we first consider the resolution due to only the finite entrance and exit slit widths of the spectrometer and consequent variation in K, then from Eq. (D4) for q=q' we have

$$q\,[\delta V_R + \delta(\Delta V/K)] = 0 \tag{D5}$$

$$\delta V_R = -\delta(\Delta V/K) \tag{D6}$$

for $q \neq q'$, for a unique value of E_G (single level) and no kinematic effects we have

$$q'[\delta V_R' + \delta(\Delta V/K)] = 0 \tag{D7}$$

$$\delta V_R' = -\delta(\Delta V/K) \tag{D8}$$

thus from (D6) and (D8)

$$\delta V_R = \delta V_R' \tag{D9}$$

Therefore the variation V_R due to the slits is the same for both the main peak and the charge exchange peak.

Now consider only a variance in the acceleration voltage V_{acc}. From Eq. (D4) for q=q' this yields

$$q\delta V_R - q\delta V_{acc} = 0 \tag{D10}$$

$$\delta V_R = \delta V_{acc} \tag{D11}$$

for $q \neq q'$

$$q'\delta V_R' - q\delta V_{acc} = 0 \tag{D12}$$

$$\delta V_R' = \frac{q}{q'}\,\delta V_{acc} \tag{D13}$$

combining (D11) and (D13) gives

$$\delta V_R' = q/q'\ \delta V_R. \tag{D14}$$

Thus the variation in V_R due to a variance in V_{acc} is different for charge exchange and main peak by a factor of q/q'.

The variations in V_R must now be changed into a E_G variation, since the spectral plots are in terms of an energy-gain. The effect due to the slits for q=q' and $q \neq q'$ from Eq. (D14) are

$$\delta E_G = q\delta V_R + q\delta(\Delta V/K) \tag{D15}$$

$$\delta E_G' = q'\delta V_R' + q'\delta(\Delta V/K). \tag{D16}$$

Dividing (D15) by (D16) and recalling Eq. (D9) yields

$$\delta E_G' = \frac{q'}{q}\,\delta E_G \tag{D17}$$

We find that due to the slits the charge exchange beam is wider than the main peak by a factor of q'/q.

We now consider the effect in $\delta E_G'$ due to a variation in V_{acc} only. From Eq. (D4) for $q=q'$

$$\delta E_G = q\delta V_R - q\delta V_{acc} \tag{D18}$$

for $q \neq q'$

$$\delta E_R' = q'\delta V_R' - q\delta V_{acc} \tag{D19}$$

recalling Eq. (D14) and dividing (D18) by (D19) yields

$$\delta E_G' = \delta E_G \tag{D20}$$

The total resolution of the system is a combination of both the slits and δV_{acc}. This can be written as

$$(\delta E_G')^2 = (\delta E_G')^2_{slits} + (\delta E_G')^2_{V_{acc}} \tag{D21}$$

Substituting Eqs. (D17) and (D20) into gives Eq. (6) from the text.

$$(\delta E_G')^2 = (\delta E_A)^2 + (\frac{q'}{q})^2\,(\delta E_S)^2 \tag{D22}$$

ELECTRON CAPTURE BY LOW-ENERGY HIGHLY-CHARGED
NEON PROJECTILES FROM HELIUM ATOMS
STUDIED BY ENERGY-GAIN SPECTROSCOPY

by

CHRIS MICHAEL SCHMEISSNER

B.S., Kansas State University, 1981

AN ABSTRACT OF A MASTER'S THESIS

submitted in partial fulfillment of the

requirements for the degree

MASTER OF SCIENCE

Department of Physics

KANSAS STATE UNIVERSITY

Manhattan, Kansas

1983

ABSTRACT

Energy-gain spectra have been measured for projectiles of Ne^{+q} (q=3-8) capturing electrons from neutral helium targets. Various projectile energies ranging from (523.53 eV·q) to (71.69 eV·q) were used for each collision system. Capture was found to populate states whose curve crossings occur near a "favored" capture radius for each collision. For capture of an electron into an orbit characterized by a principle quantum number n, no preferential population of a particular ℓ was found. This "favored" radius for capture is determined systematically with the use of an empirically determined coupling matrix element.